Chapter 8

Particles Widely Separated: The Method of Reflections

8.1 The Far Field

A quite general asymptotic method valid for particles of arbitrary shape is at our disposal for two widely separated particles (large R/a, where R is the particle-particle separation and a is the characteristic particle size). This perturbation scheme in small a/R was developed by Smoluchowski [64] and has come to be known as the *method of reflections* [27]. A recent work by Luke [54] furnishes a proof based on energy dissipation arguments that the scheme converges for particles of quite general shape. (See also the discussion at the end of Chapter 15.)

In the zeroeth order approximation, the solution for two widely separated particles is formed by superposition of the fields produced by the isolated particle solutions. In other words, we neglect hydrodynamic interactions between particles. We have seen earlier in Chapter 3 that the disturbance field of an isolated particle may be written as a multipole expansion and that such an expansion is particularly useful in the analysis of the far field. The method of reflections is based on the idea that the ambient field about each particle consists of the original ambient field plus the disturbance field produced by the other particle(s). The method is iterative, since a correction of the ambient field about a given particle generates a new disturbance solution for that particle, which in turn modifies the ambient field about another particle.

The process of incorporating the effect of an ambient field with a new disturbance field is called a *reflection*, hence the name, *method of reflections*. The ambient field used in the reflection is denoted as the *incident* field, and the new disturbance solution is denoted as the *reflected* field. The solution procedure may be envisioned as illustrated in Figure 8.1.

For the two-particle problem, we take $\boldsymbol{x}_1$ and $\boldsymbol{x}_2$ as the reference positions for each particle and denote the isolated particle solutions as $\boldsymbol{v}_1$ and $\boldsymbol{v}_2$. Now on the surfaces S_1 and S_2 of each particle, we have the boundary conditions,

$$\boldsymbol{v}_1 = \boldsymbol{U}_1 + \boldsymbol{\omega}_1 \times (\boldsymbol{x} - \boldsymbol{x}_1) - \boldsymbol{v}^\infty \quad \text{on } S_1$$

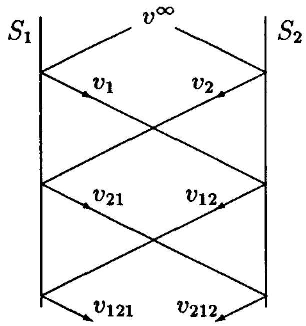

Figure 8.1: Schematic diagram of the method of reflections for two particles.

$$\boldsymbol{v}_2 = \boldsymbol{U}_2 + \boldsymbol{\omega}_2 \times (\boldsymbol{x} - \boldsymbol{x}_2) - \boldsymbol{v}^{\infty} \quad \text{on } S_2 ,$$

and so if we set $\boldsymbol{v} = \boldsymbol{v}^{\infty} + \boldsymbol{v}_1 + \boldsymbol{v}_2$, we see that the errors in the boundary condition follow as $\boldsymbol{v}_2(x)$ for a point x on the surface of particle 1 and $\boldsymbol{v}_1(x)$ for a point on particle 2. This error will be at least as small as a/R, since the decay in $\boldsymbol{v}_1$ and $\boldsymbol{v}_2$ is at most that of a Stokes monopole. The next reflection will reduce this error.

The first reflection fields $\boldsymbol{v}_{12}$ and $\boldsymbol{v}_{21}$ are defined formally as the solutions to the Stokes equations vanishing at infinity with the additional boundary conditions

$$\begin{aligned} \boldsymbol{v}_{12} &= -\boldsymbol{v}_1 && \text{on } S_2 \\ \boldsymbol{v}_{21} &= -\boldsymbol{v}_2 && \text{on } S_1 . \end{aligned}$$

Now the errors in the boundary condition scale as $\boldsymbol{v}_{12}(\boldsymbol{x})$ for a point $\boldsymbol{x}$ on the surface of particle 1 and $\boldsymbol{v}_{21}(\boldsymbol{x})$ for a point on particle 2. The error has been reduced, since the the far field values of $\boldsymbol{v}_{12}(\boldsymbol{x})$ and $\boldsymbol{v}_{21}(\boldsymbol{x})$ are smaller than the near field values of the same, and these in turn are of the same order of magnitude as the far field values of $\boldsymbol{v}_2(\boldsymbol{x})$ and $\boldsymbol{v}_1(\boldsymbol{x})$.

The higher order reflections are obtained in exactly the same manner. For example, the next reflections are obtained with $\boldsymbol{v}_{12}$ and $\boldsymbol{v}_{21}$ playing the roles previously played by $\boldsymbol{v}_2$ and $\boldsymbol{v}_1$. The reflected fields will be denoted by $\boldsymbol{v}_{121}$ and $\boldsymbol{v}_{212}$. In general, we shall keep track of all fields by assigning unique subscripts formed by augmenting the subscripts of the incident field by the subscript corresponding to the particle on which the reflection is taking place. The error in the boundary condition is given by the values taken by the highest order reflected fields evaluated at the surface of the other particle (which is also a far field value).

Finally, the most natural form for the reflected fields is the multipole expansion, with the moments determined by application of the Faxén law (on the incident fields). For simple shapes such as spheres and ellipsoids, analytical forms of the Faxén laws are available (Chapter 3), and so the method of reflections will yield analytical solutions. For the general particle shape, the Faxén relations are obtained by applying the reciprocal theorem to the dual boundary value problem. If the latter are obtained from a numerical solution, then the method of reflections will yield semi-analytical solutions, since the coefficients in the a/R expansion originate from the numerical solutions.

We now examine the formal structure of the method of reflections, in particular the differences in the method as applied to resistance problems and mobility problems. While the method works equally well for both problems, for two reasons its main application in microhydrodynamics lies in mobility problems. First, mobility problems arise more frequently in microhydrodynamics and the method produces the desired solutions directly, *i.e.*, without an inversion of the resistance problem. The second reason is that the far field forms of the mobility functions are quite accurate, even when the particles are fairly close together. The reason, as we shall see shortly, is that the higher order reflections in mobility problems consist of dipole-dipole interactions, which are much weaker than the monopole-monopole interactions usually encountered in resistance problems.

8.2 Resistance Problems

In resistance problems, particle motions and the ambient field are prescribed, and we must determine the force, torque, and higher order moments of the surface traction. Also, the zeroeth order fields $\boldsymbol{v}_1$ and $\boldsymbol{v}_2$ produce exactly, the prescribed particle motions. In subsequent reflections, the reflected fields satisfy the no-slip condition. Thus at each reflection, the multipole expansion for the reflected field always leads off with a Stokes monopole. The strength of the Stokes monopole, *i.e.*, the hydrodynamic force on the particle, always scales as the difference between the ambient velocity and the particle velocity. Since the latter is zero at the higher order reflections, the strength of the monopole will be equal to the magnitude of the incident field, which in turn is simply the far field limit of the previous reflection. Thus in resistance problems we typically get the following behavior:

$$\boldsymbol{F}_\alpha^{(n+1)} \sim O\left(\frac{a}{R}\right) \boldsymbol{F}_\beta^{(n)} ;$$

the $(n+1)$-th reflection's contribution to the hydrodynamic force on particle α will be $O(a/R)$ smaller than n-th reflection's contribution to particle β. In particular, for flow past two stationary bodies, we have

$$\boldsymbol{F}_\alpha^{(N)} \sim O\left(\frac{a}{R}\right)^N .$$

The scaling for other moments, such as the torque and stresslet, may be obtained by reference to the Faxén relations; the end result is that for a given reflection, the n-th moment of the surface traction is $O(a/R)$ smaller than the $(n-1)$-th order moment. In actual applications we must first set the desired order of accuracy in a/R. This then will determine how many multipole moments are required, with the number of required moments going down as the order of the reflection is raised. These ideas are illustrated in the following examples on resistance problems for spheres.

Example 8.1 Resistance Tensors for Two Translating Spheres.
We take two nonrotating spheres centered at $\boldsymbol{x}_1$ and $\boldsymbol{x}_2$, with radii a and b, and translational velocities $\boldsymbol{U}_1$ and $\boldsymbol{U}_2$, respectively. We define the parameter $\beta = b/a$ for the ratio of sphere radii. Our goal is to calculate the force, torque, and stresslet on the spheres, accurate to $O(R^{-4})$.

The zeroeth order solution is simply the Stokes solution for the disturbance caused by an isolated, translating sphere in a uniform stream. Thus we have

$$\begin{aligned}
\boldsymbol{v}_1 &= -\boldsymbol{F}_1^{(0)} \cdot \left\{1 + \frac{a^2}{6}\nabla^2\right\} \frac{\mathcal{G}(\boldsymbol{x}-\boldsymbol{x}_1)}{(8\pi\mu)} \\
\boldsymbol{v}_2 &= -\boldsymbol{F}_2^{(0)} \cdot \left\{1 + \frac{b^2}{6}\nabla^2\right\} \frac{\mathcal{G}(\boldsymbol{x}-\boldsymbol{x}_2)}{(8\pi\mu)} ,
\end{aligned}$$

with

$$\begin{aligned}
\boldsymbol{F}_1^{(0)} &= 6\pi\mu a(\boldsymbol{U}^\infty - \boldsymbol{U}_1) \\
\boldsymbol{T}_1^{(0)} &= 0 \\
\boldsymbol{S}_1^{(0)} &= 0 ,
\end{aligned}$$

and a similar set of results for sphere 2.

The first reflection fields, $\boldsymbol{v}_{21}$ and $\boldsymbol{v}_{12}$, are expanded as

$$\begin{aligned}
\boldsymbol{v}_{21} &= -\boldsymbol{F}_1^{(1)} \cdot \left\{1 + \frac{a^2}{6}\nabla^2\right\} \frac{\mathcal{G}(\boldsymbol{x}-\boldsymbol{x}_1)}{(8\pi\mu)} \\
&\quad + \left[\boldsymbol{S}_1^{(1)} \cdot \nabla + \frac{1}{2}\boldsymbol{T}_1^{(1)} \times \nabla\right] \cdot \frac{\mathcal{G}(\boldsymbol{x}-\boldsymbol{x}_1)}{(8\pi\mu)} + \cdots \\
\boldsymbol{v}_{12} &= -\boldsymbol{F}_2^{(1)} \cdot \left\{1 + \frac{b^2}{6}\nabla^2\right\} \frac{\mathcal{G}(\boldsymbol{x}-\boldsymbol{x}_2)}{(8\pi\mu)} \\
&\quad + \left[\boldsymbol{S}_2^{(1)} \cdot \nabla + \frac{1}{2}\boldsymbol{T}_2^{(1)} \times \nabla\right] \cdot \frac{\mathcal{G}(\boldsymbol{x}-\boldsymbol{x}_2)}{(8\pi\mu)} + \cdots ,
\end{aligned}$$

with multipole moments obtained from the Faxén laws as

$$\begin{aligned}
\boldsymbol{F}_1^{(1)} &= 6\pi\mu a(1 + \frac{a^2}{6}\nabla^2)\boldsymbol{v}_2|_{x=x_1} \\
&= \boldsymbol{F}_2^{(0)} \cdot \left[\left(-\frac{3}{2}\frac{a}{R} + \frac{1}{2}(1+\beta^2)\left(\frac{a}{R}\right)^3\right)\boldsymbol{dd}\right. \\
&\quad \left. - \left(\frac{3}{4}\frac{a}{R} + \frac{1}{4}(1+\beta^2)\left(\frac{a}{R}\right)^3\right)(\boldsymbol{\delta} - \boldsymbol{dd})\right]
\end{aligned}$$

$$\begin{aligned}
\boldsymbol{T}_1^{(1)} &= 4\pi\mu a^3 \nabla \times \boldsymbol{v}_2|_{x=x_1} \\
&= \frac{a^3}{R^2}\boldsymbol{F}_2^{(0)} \times \boldsymbol{d} \\
\boldsymbol{S}_1^{(1)} &= \frac{20}{3}\pi\mu a^3 (1 + \frac{a^2}{10}\nabla^2)\boldsymbol{e}_2|_{x=x_1} \\
&= \left(-\frac{5}{2}\frac{a^3}{R^2} + \frac{3}{2}\frac{a^5}{R^4}(1+\frac{5}{3}\beta^2)\right)(\boldsymbol{dd} - \frac{1}{3}\boldsymbol{\delta})\boldsymbol{d}\cdot\boldsymbol{F}_2^{(0)} \\
&- \frac{1}{2}\frac{a^5}{R^4}(1+\frac{5}{3}\beta^2)(\boldsymbol{F}_2^{(0)}\boldsymbol{d} + \boldsymbol{d}\boldsymbol{F}_2^{(0)} - 2\boldsymbol{ddd}\cdot\boldsymbol{F}_2^{(0)})\ .
\end{aligned}$$

Here, $\boldsymbol{d}$ denotes the unit vector, $(\boldsymbol{x}_2 - \boldsymbol{x}_1)/|\boldsymbol{x}_2 - \boldsymbol{x}_1|$. The algebraic reductions were obtained by inserting the appropriate expressions for $\mathcal{G}$ and its derivatives. Note that $\boldsymbol{T}^{(1)}$ does not have a term of $O(R^{-4})$ because $\nabla^2\mathcal{G}$ is irrotational. Expressions for $\boldsymbol{F}_2^{(1)}$, $\boldsymbol{T}_2^{(1)}$, and $\boldsymbol{S}_2^{(1)}$ may be obtained from the preceding by switching a and b and the indices 1 and 2.

At the next (second) reflection the fields $\boldsymbol{v}_{121}$ and $\boldsymbol{v}_{212}$ are expanded as

$$\begin{aligned}
\boldsymbol{v}_{121} &= -\boldsymbol{F}_1^{(2)}\cdot\left\{1 + \frac{a^2}{6}\nabla^2\right\}\frac{\mathcal{G}(\boldsymbol{x}-\boldsymbol{x}_1)}{(8\pi\mu)} \\
&+ \left[\boldsymbol{S}_1^{(2)}\cdot\nabla + \frac{1}{2}\boldsymbol{T}_1^{(2)}\times\nabla\right]\cdot\frac{\mathcal{G}(\boldsymbol{x}-\boldsymbol{x}_1)}{(8\pi\mu)} + \cdots \\
\boldsymbol{v}_{212} &= -\boldsymbol{F}_2^{(2)}\cdot\left\{1 + \frac{b^2}{6}\nabla^2\right\}\frac{\mathcal{G}(\boldsymbol{x}-\boldsymbol{x}_2)}{(8\pi\mu)} \\
&+ \left[\boldsymbol{S}_2^{(2)}\cdot\nabla + \frac{1}{2}\boldsymbol{T}_2^{(2)}\times\nabla\right]\cdot\frac{\mathcal{G}(\boldsymbol{x}-\boldsymbol{x}_2)}{(8\pi\mu)} + \cdots\ ,
\end{aligned}$$

with multipole moments obtained from the Faxén laws as

$$\begin{aligned}
\boldsymbol{F}_1^{(2)} &= 6\pi\mu a(1 + \frac{a^2}{6}\nabla^2)\boldsymbol{v}_{12}|_{x=x_1} \\
&= \boldsymbol{F}_2^{(1)}\cdot\left[\left(-\frac{3}{2}\frac{a}{R} + \frac{1}{2}(1+\beta^2)\left(\frac{a}{R}\right)^3\right)\boldsymbol{dd}\right. \\
&- \left.\left(\frac{3}{4}\frac{a}{R} + \frac{1}{4}(1+\beta^2)\left(\frac{a}{R}\right)^3\right)(\boldsymbol{\delta} - \boldsymbol{dd})\right] \\
&= \boldsymbol{F}_1^{(0)}\cdot\left[\left(\frac{9}{4}\beta\left(\frac{a}{R}\right)^2 - (\frac{3\beta}{2} + \frac{3\beta^3}{4})\left(\frac{a}{R}\right)^4\right)\boldsymbol{dd}\right. \\
&+ \left.\left(\frac{9}{16}\beta\left(\frac{a}{R}\right)^2 + (\frac{3\beta}{8} + \frac{3\beta^3}{16})\left(\frac{a}{R}\right)^4\right)(\boldsymbol{\delta} - \boldsymbol{dd})\right] \\
\boldsymbol{T}_1^{(2)} &= 4\pi\mu a^3\nabla \times \boldsymbol{v}_{12}|_{x=x_1} \\
&= \frac{a^3}{R^2}\boldsymbol{F}_2^{(1)} \times \boldsymbol{d} \\
&= -\frac{3\beta}{4}\frac{a^4}{R^3}\boldsymbol{F}_1^{(0)} \times \boldsymbol{d} + O(R^{-5})
\end{aligned}$$

$$\begin{aligned}
S_1^{(2)} &= \frac{20}{3}\pi\mu a^3(1+\frac{a^2}{10}\nabla^2)e_{12}|_{x=x_1} \\
&= -\frac{5}{2}\frac{a^3}{R^2}(dd-\frac{1}{3}\delta)d\cdot F_2^{(1)} + O(R^{-5}) \\
&= \frac{15\beta}{4}\frac{a^4}{R^3}(dd-\frac{1}{3}\delta)d\cdot F_1^{(0)} + O(R^{-5})\ .
\end{aligned}$$

As before, expressions for $F_2^{(2)}$, $T_2^{(2)}$, and $S_2^{(2)}$ may be obtained from the analogous quantity for sphere 1 by switching a and b and the indices 1 and 2.

Since the final results are desired accurate to $O(R^{-4})$, the contributions from the third and fourth reflections may be obtained by retaining only the leading order (Stokes monopole) terms at the earlier reflections. The results are

$$\begin{aligned}
F_1^{(3)} &= \left(-\frac{3a}{4}\mathcal{G}(x_1-x_2)\right)\cdot\left(-\frac{3b}{4}\mathcal{G}(x_2-x_1)\right)\cdot\left(-\frac{3a}{4}\mathcal{G}(x_1-x_2)\right)\cdot F_2^0 \\
&= -F_2^{(0)}\cdot\left[\frac{27\beta}{8}\left(\frac{a}{R}\right)^3 dd + \frac{27\beta}{64}\left(\frac{a}{R}\right)^3(\delta-dd)\right] \\
T_1^{(3)} &= \frac{9\beta}{16}\frac{a^5}{R^4}F_2^{(0)}\times d + O(R^{-6}) \\
S_1^{(3)} &= -\frac{45\beta}{32}\frac{a^5}{R^4}(dd-\frac{1}{3}\delta)d\cdot F_2^{(0)} + O(R^{-6})
\end{aligned}$$

and

$$\begin{aligned}
F_1^{(4)} &= \left(-\frac{3a}{4}\mathcal{G}(x_1-x_2)\right)\cdot\left(-\frac{3b}{4}\mathcal{G}(x_2-x_1)\right)\cdot\left(-\frac{3a}{4}\mathcal{G}(x_1-x_2)\right) \\
&\quad\cdot\left(-\frac{3b}{4}\mathcal{G}(x_2-x_1)\right)\cdot F_1^0 \\
&= F_1^{(0)}\cdot\left[\frac{81\beta^2}{16}\left(\frac{a}{R}\right)^4 dd + \frac{81\beta^2}{256}\left(\frac{a}{R}\right)^4(\delta-dd)\right] \\
T_1^{(4)} &\sim O(R^{-5}) \\
S_1^{(4)} &\sim O(R^{-5})\ .
\end{aligned}$$

The combined result for F_1, T_1, and S_1 obtained by adding the contributions from the zeroeth through the fourth reflection is

$$\begin{aligned}
F_1 &= F_1^{(0)}\cdot\left[\left(1+\frac{9}{4}\beta\left(\frac{a}{R}\right)^2 - (\frac{3\beta}{2}+\frac{81\beta^2}{16}+\frac{3\beta^3}{4})\left(\frac{a}{R}\right)^4\right)dd\right. \\
&\quad\left. + \left(1+\frac{9}{16}\beta\left(\frac{a}{R}\right)^2 + (\frac{3\beta}{8}-\frac{81\beta^2}{256}+\frac{3\beta^3}{16})\left(\frac{a}{R}\right)^4\right)(\delta-dd)\right] \\
&+ F_2^{(0)}\cdot\left[\left(-\frac{3}{2}\frac{a}{R}+\frac{1}{2}(1-\frac{27\beta}{4}+\beta^2)\left(\frac{a}{R}\right)^3\right)dd\right. \\
&\quad\left. - \left(\frac{3}{4}\frac{a}{R}+\frac{1}{4}(1+\frac{27\beta}{16}+\beta^2)\left(\frac{a}{R}\right)^3\right)(\delta-dd)\right]
\end{aligned}$$

$$
\begin{aligned}
\boldsymbol{T}_1 &= -\frac{3\beta}{4}\frac{a^4}{R^3}\boldsymbol{F}_1^{(0)} \times \boldsymbol{d} + \left(\frac{a^3}{R^2} + \frac{9\beta}{16}\frac{a^5}{R^4}\right)\boldsymbol{F}_2^{(0)} \times \boldsymbol{d} \\
\boldsymbol{S}_1 &= \frac{15\beta}{4}\frac{a^4}{R^3}(\boldsymbol{dd} - \frac{1}{3}\boldsymbol{\delta})\boldsymbol{d} \cdot \boldsymbol{F}_1^{(0)} \\
&+ \left(-\frac{5}{2}\frac{a^3}{R^2} + \frac{3}{2}(1 - \frac{15\beta}{16} + \frac{5\beta^2}{3})\frac{a^5}{R^4}\right)(\boldsymbol{dd} - \frac{1}{3}\boldsymbol{\delta})\boldsymbol{d} \cdot \boldsymbol{F}_2^{(0)} \\
&- \frac{1}{2}(1 + \frac{5}{3}\beta^2)\frac{a^5}{R^4}(\boldsymbol{F}_2^{(0)}\boldsymbol{d} + \boldsymbol{d}\boldsymbol{F}_2^{(0)} - 2\boldsymbol{ddd} \cdot \boldsymbol{F}_2^{(0)}) \ ,
\end{aligned}
$$

which is consistent with the forms obtained for axisymmetric geometries in the previous chapter ◇

The preceding example illustrates the general statements made earlier about the method of reflections. Later on we shall consider a much more efficient implementation of the method of reflection for spheres that is based on the addition theorem for spherical harmonics.

We know quite a bit about pair interactions. It would be very convenient if multiparticle interactions could be described in a pairwise-additive fashion. In the next example, we solve a three-body problem by the method of reflections, and find that three-body effects come in at $O(a/R)^2$. This is a fairly strong interaction, which implies that pairwise addition of the resistance functions is not as accurate as the corresponding treatments in molecular simulations.

Example 8.2 Three-Body Effects.
Consider three identical, fixed, nonrotating spheres with centers at $\boldsymbol{x}_1$, $\boldsymbol{x}_2$, and $\boldsymbol{x}_3$, in a uniform stream $\boldsymbol{U}^\infty$. We can easily generalize the analysis to handle unequal spheres. As in the two-sphere problem, we label reflection fields by appending the sphere-number to the label of the incident field.

The zeroeth order solution is simply the linear superposition of the three Stokes solutions:

$$
\begin{aligned}
\boldsymbol{v}_1 &= -\boldsymbol{F}^{(0)} \cdot \left\{1 + \frac{a^2}{6}\nabla^2\right\}\frac{\mathcal{G}(\boldsymbol{x} - \boldsymbol{x}_1)}{(8\pi\mu)} \\
\boldsymbol{v}_2 &= -\boldsymbol{F}^{(0)} \cdot \left\{1 + \frac{a^2}{6}\nabla^2\right\}\frac{\mathcal{G}(\boldsymbol{x} - \boldsymbol{x}_2)}{(8\pi\mu)} \\
\boldsymbol{v}_3 &= -\boldsymbol{F}^{(0)} \cdot \left\{1 + \frac{a^2}{6}\nabla^2\right\}\frac{\mathcal{G}(\boldsymbol{x} - \boldsymbol{x}_3)}{(8\pi\mu)} \ ,
\end{aligned}
$$

with

$$
\boldsymbol{F}^{(0)} = 6\pi\mu a \boldsymbol{U}^\infty \ .
$$

There are six reflection fields — $\boldsymbol{v}_{21}$, $\boldsymbol{v}_{31}$, $\boldsymbol{v}_{12}$, $\boldsymbol{v}_{32}$, $\boldsymbol{v}_{13}$, and $\boldsymbol{v}_{23}$ — at the next reflection, since each sphere sees incident fields from two sources. The expression for $\boldsymbol{v}_{21}$ is identical to that encountered in the two-sphere problem:

$$
\begin{aligned}
\boldsymbol{v}_{21} &= -\boldsymbol{F}_1^{(2)} \cdot \left\{1 + \frac{a^2}{6}\nabla^2\right\}\frac{\mathcal{G}(\boldsymbol{x} - \boldsymbol{x}_1)}{(8\pi\mu)} \\
&+ \left[\boldsymbol{S}_1^{(2)} \cdot \nabla + \frac{1}{2}\boldsymbol{T}_1^{(2)} \times \nabla\right] \cdot \frac{\mathcal{G}(\boldsymbol{x} - \boldsymbol{x}_1)}{(8\pi\mu)} + \cdots \ ,
\end{aligned}
$$

with multipole moments[1] obtained from the Faxén laws as

$$
\begin{aligned}
\boldsymbol{F}_1^{(2)} &= 6\pi\mu a(1+\frac{a^2}{6}\nabla^2)\boldsymbol{v}_2|_{x=x_1} \\
&= \boldsymbol{F}^{(0)}\cdot\left[\left(-\frac{3}{2}\frac{a}{R_{12}}+\left(\frac{a}{R_{12}}\right)^3\right)\boldsymbol{d}_{12}\boldsymbol{d}_{12}\right. \\
&\quad \left. -\left(\frac{3}{4}\frac{a}{R_{12}}+\frac{1}{2}\left(\frac{a}{R_{12}}\right)^3\right)(\boldsymbol{\delta}-\boldsymbol{d}_{12}\boldsymbol{d}_{12})\right] \\
\boldsymbol{T}_1^{(2)} &= 4\pi\mu a^3\nabla\times\boldsymbol{v}_2|_{x=x_1} \\
&= \frac{a^3}{R_{12}^2}\boldsymbol{F}^{(0)}\times\boldsymbol{d}_{12} \\
\boldsymbol{S}_1^{(2)} &= \frac{20}{3}\pi\mu a^3(1+\frac{a^2}{10}\nabla^2)\boldsymbol{e}_2|_{x=x_1} \\
&= \left(-\frac{5}{2}\frac{a^3}{R_{12}^2}+4\frac{a^5}{R_{12}^4}\right)(\boldsymbol{d}_{12}\boldsymbol{d}_{12}-\frac{1}{3}\boldsymbol{\delta})\boldsymbol{d}_{12}\cdot\boldsymbol{F}^{(0)} \\
&\quad -\frac{4}{3}\frac{a^5}{R_{12}^4}(\boldsymbol{F}^{(0)}\boldsymbol{d}_{12}+\boldsymbol{d}_{12}\boldsymbol{F}^{(0)}-2\boldsymbol{d}_{12}\boldsymbol{d}_{12}\boldsymbol{d}_{12}\cdot\boldsymbol{F}^{(0)})\ ,
\end{aligned}
$$

with $R_{12}=|\boldsymbol{x}_1-\boldsymbol{x}_2|$ and $\boldsymbol{d}_{12}=(\boldsymbol{x}_1-\boldsymbol{x}_2)/R_{12}$. The corresponding expressions for the other five reflection fields may be obtained from these expressions by the appropriate permutation of sphere labels. Note that three-body effects have not entered at this order (each quantity has at most two of the three sphere labels).

At the next (second) reflection, let us examine only reflections at sphere 1, with the understanding that the same events occur at spheres 2 and 3. Of the six first-reflection fields, only the four that emanate from either sphere 2 or 3 may act as incident fields on sphere 1. For each incident field, we have a reflection field, namely, $\boldsymbol{v}_{121}$, $\boldsymbol{v}_{131}$, $\boldsymbol{v}_{231}$, and $\boldsymbol{v}_{321}$. The last two are three-body effects and we see that if $R_{12}\sim R_{13}\sim R_{23}\sim R$, then three-body effects come in at $O(R^{-2})$.

For each reflection field, we use the multipole expansion, with moments determined from Faxén laws. The expressions for $\boldsymbol{v}_{121}$ and $\boldsymbol{v}_{231}$ are given below:

$$
\begin{aligned}
\boldsymbol{v}_{121} &= -\boldsymbol{F}_1^{(12)}\cdot\left\{1+\frac{a^2}{6}\nabla^2\right\}\frac{\mathcal{G}(\boldsymbol{x}-\boldsymbol{x}_1)}{(8\pi\mu)} \\
&\quad +\left[\boldsymbol{S}_1^{(12)}\cdot\nabla+\frac{1}{2}\boldsymbol{T}_1^{(12)}\times\nabla\right]\cdot\frac{\mathcal{G}(\boldsymbol{x}-\boldsymbol{x}_1)}{(8\pi\mu)}+\cdots\ ,
\end{aligned}
$$

with

$$
\begin{aligned}
\boldsymbol{F}_1^{(12)} &= 6\pi\mu a(1+\frac{a^2}{6}\nabla^2)\boldsymbol{v}_{12}|_{x=x_1} \\
\boldsymbol{T}_1^{(12)} &= 4\pi\mu a^3\nabla\times\boldsymbol{v}_{12}|_{x=x_1} \\
\boldsymbol{S}_1^{(12)} &= \frac{20}{3}\pi\mu a^3(1+\frac{a^2}{10}\nabla^2)\boldsymbol{e}_{12}|_{x=x_1}\ ,
\end{aligned}
$$

[1]In the three-sphere problem, we depart from the convention used earlier and indicate the reflection order by using the same label as the incident field.

$$
\begin{aligned}
v_{231} &= -F_1^{(23)} \cdot \left\{1 + \frac{a^2}{6}\nabla^2\right\} \frac{\mathcal{G}(x - x_1)}{(8\pi\mu)} \\
&\quad + \left[S_1^{(23)} \cdot \nabla + \frac{1}{2}T_1^{(23)} \times \nabla\right] \cdot \frac{\mathcal{G}(x - x_1)}{(8\pi\mu)} + \cdots ,
\end{aligned}
$$

with

$$
\begin{aligned}
F_1^{(23)} &= 6\pi\mu a(1 + \frac{a^2}{6}\nabla^2) v_{23}|_{x=x_1} \\
T_1^{(23)} &= 4\pi\mu a^3 \nabla \times v_{23}|_{x=x_1} \\
S_1^{(23)} &= \frac{20}{3}\pi\mu a^3 (1 + \frac{a^2}{10}\nabla^2) e_{23}|_{x=x_1} .
\end{aligned}
$$

The expressions for v_{131} and v_{321} are obtained in a similar manner.

The force on sphere 1 may be written as

$$
\begin{aligned}
F_1 &= 6\pi\mu a U^{\infty} + F_1^{(2)} + F_1^{(3)} \\
&\quad + F_1^{(12)} + F_1^{(13)} + F_1^{(23)} + F_1^{(32)} \\
&\quad + F_1^{(123)} + F_1^{(132)} + \ldots + F_1^{(323)} \\
&\quad + F_1^{(1212)} + F_1^{(1232)} + \ldots + F_1^{(3213)} \\
&\quad + F_1^{(12123)} + F_1^{(12132)} + \ldots + F_1^{(32323)} ,
\end{aligned}
$$

where the contributions from the zeroeth through the fifth reflection are as indicated. The tracking of the reflection fields (there are $3 \times 2^{n+1}$ fields at the n-th reflection) is a straightforward exercise in bookkeeping skills; the essential aspects of the method differ very little from that encountered earlier in the two-sphere problem.

For spheres centered at the vertices of an equilateral triangle (so that $R_{12} = R_{13} = R_{23} = R$, see Figure 8.2), the final result is quite simple, since the single parameter R/a describes the problem geometry, and the force on sphere 1 may be written as [46]

$$
F_1 = 6\pi\mu a U^{\infty} \cdot [f_1 e_1 e_1 + f_2 e_2 e_2 + f_3 e_3 e_3] ,
$$

with

$$
e_1 = \frac{1}{\sqrt{3}}(d_{12} + d_{13}) , \qquad e_2 = d_{23} , \qquad e_3 = e_1 \times e_2 ,
$$

and

$$
\begin{aligned}
f_1 &= 1 - \frac{21}{8}\left(\frac{a}{R}\right) + \frac{45}{8}\left(\frac{a}{R}\right)^2 - \frac{6191}{512}\left(\frac{a}{R}\right)^3 + \frac{135327}{4096}\left(\frac{a}{R}\right)^4 \\
&\quad - \frac{689823}{8192}\left(\frac{a}{R}\right)^5 + \cdots \\
f_2 &= 1 - \frac{15}{8}\left(\frac{a}{R}\right) + \frac{153}{32}\left(\frac{a}{R}\right)^2 - \frac{5447}{512}\left(\frac{a}{R}\right)^3 + \frac{102885}{4096}\left(\frac{a}{R}\right)^4 \\
&\quad - \frac{1085373}{16384}\left(\frac{a}{R}\right)^5 + \cdots \\
f_3 &= 1 - \frac{3}{2}\left(\frac{a}{R}\right) + \frac{9}{4}\left(\frac{a}{R}\right)^2 - \frac{35}{8}\left(\frac{a}{R}\right)^3 + \frac{165}{16}\left(\frac{a}{R}\right)^4 - \frac{675}{32}\left(\frac{a}{R}\right)^5 + \cdots
\end{aligned}
$$

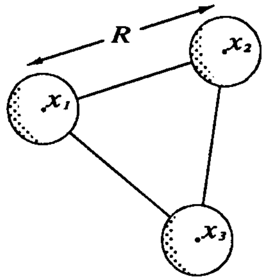

Figure 8.2: The three-sphere geometry.

The effects of three-body interactions are shown in Figure 8.2, where these results are plotted along with the pairwise additive approximations. In general, resistance functions are not pairwise additive in the far field. In Exercise 8.3, the corresponding mobility problem is considered, and the reader will see that the analysis is considerably easier. ◇

8.3 Mobility Problems

In mobility problems, particle motions in a specified ambient field are to be determined. The motions arise from prescribed forces and torques on each particle. We may also want to calculate higher order moments of the traction such as the stresslet. As in the resistance problem, we start with the single-particle solutions $\boldsymbol{v}_1$ and $\boldsymbol{v}_2$, but in the reflection procedure there are essential differences.

In mobility problems, the zeroeth order fields $\boldsymbol{v}_1$ and $\boldsymbol{v}_2$ produce exactly the *prescribed forces and torques.* Therefore, in subsequent reflections the particle motions must be such that the reflected fields are force-free and torque-free. These translational and rotational velocities will scale as the ambient velocity and velocity gradient, respectively. Furthermore, the reflected field's multipole expansion will lead off with a *stresslet* of strength of the same order as the ambient velocity gradient. Thus in mobility problems we typically get the following behavior:

$$\boldsymbol{U}_\alpha^{(N+1)} \sim O\left(\frac{a}{R}\right)^3 \boldsymbol{U}_\beta^{(N)} ,$$

that is, the $(N+1)$-th reflection's contribution to the translational velocity of particle α will be $O(a/R)^3$ smaller than the N-th reflection's contribution to the velocity of particle β. Two powers of a/R are due to the far field decay of the stresslet field, while the additional factor of a/R is due to the relative magnitudes of $\boldsymbol{U}_\beta^{(N)}$ and $\boldsymbol{S}_\beta^{(N)}$. The scaling for other higher order moments of

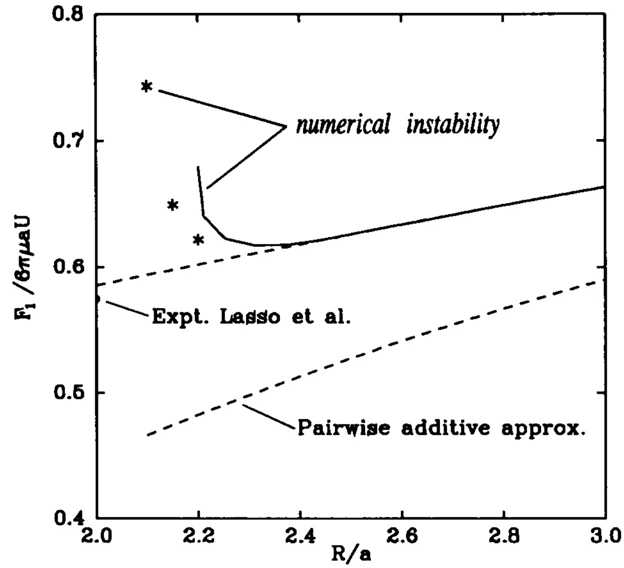

Figure 8.3: Three-sphere interactions and pairwise additive approximations.

the traction is as before and the n-th moment of the surface traction will be $O(a/R)$ smaller than the $(n-1)$-th order moment.

The end result is that, *given the same amount of information concerning the Faxén relations for the moments, and after the same number of reflections, the results for the mobility functions will be accurate to higher order in a/R than the result for the resistance functions.* Thus, contrary to one's initial perception and the approach in the older literature, when applying the method of reflections, one should first solve the entire collection of mobility problems and then invert these if the resistance solutions are also required. These ideas will be illustrated with the mobility calculation for spheres. We will perform the same number of reflections as in the resistance problem, but will obtain solutions accurate to $O(a/R)^7$. These may then be inverted to obtain the resistance relations accurate to $O(a/R)^7$.

Example 8.3 Two Torque-Free Spheres Acted on by External Forces in a Quiescent Fluid.
We shall derive, accurate to $O(R^{-5})$, and errors of $O(R^{-7})$, the translational and rotational velocities of two torque-free spheres acted on by external forces in a quiescent fluid (this includes the sedimentation problem).

We take two spheres centered at $\boldsymbol{x}_1$ and $\boldsymbol{x}_2$, with radii a and b, and denote the external forces as $\boldsymbol{F}_1^e$ and $\boldsymbol{F}_2^e$, respectively. As in the resistance problem, we define $\beta = b/a$. The zeroeth order solution is the Stokes solution for an isolated, translating sphere, *i.e.*,

$$\begin{aligned} \boldsymbol{v}_1 &= \boldsymbol{F}_1^e \cdot \left\{1 + \frac{a^2}{6}\nabla^2\right\} \frac{\mathcal{G}(\boldsymbol{x}-\boldsymbol{x}_1)}{(8\pi\mu)} \\ \boldsymbol{v}_2 &= \boldsymbol{F}_2^e \cdot \left\{1 + \frac{b^2}{6}\nabla^2\right\} \frac{\mathcal{G}(\boldsymbol{x}-\boldsymbol{x}_2)}{(8\pi\mu)} , \end{aligned}$$

with

$$\begin{aligned} 6\pi\mu a \boldsymbol{U}_1^{(0)} &= \boldsymbol{F}_1^e = -\boldsymbol{F}_1 \\ \boldsymbol{T}_1^{(0)} &= 0 \\ 6\pi\mu b \boldsymbol{U}_2^{(0)} &= \boldsymbol{F}_2^e = -\boldsymbol{F}_2 \\ \boldsymbol{T}_2^{(0)} &= 0 . \end{aligned}$$

The first reflection fields, $\boldsymbol{v}_{21}$ and $\boldsymbol{v}_{12}$, are expanded as

$$\begin{aligned} \boldsymbol{v}_{21} &= (\boldsymbol{S}_1^{(1)} \cdot \nabla) \cdot \frac{\mathcal{G}(\boldsymbol{x}-\boldsymbol{x}_1)}{(8\pi\mu)} + \cdots \\ \boldsymbol{v}_{12} &= (\boldsymbol{S}_2^{(1)} \cdot \nabla) \cdot \frac{\mathcal{G}(\boldsymbol{x}-\boldsymbol{x}_2)}{(8\pi\mu)} + \cdots , \end{aligned}$$

with particle motions and stresslets obtained from the Faxén laws as

$$\begin{aligned} \boldsymbol{U}_1^{(1)} &= (1 + \frac{a^2}{6}\nabla^2)\boldsymbol{v}_2|_{x=x_1} \\ &= \boldsymbol{U}_2^{(0)} \cdot \left[\left(\frac{3\beta}{2}\frac{a}{R} - \frac{1}{2}\beta(1+\beta^2)\left(\frac{a}{R}\right)^3\right)\boldsymbol{dd} \right. \\ &\quad \left. + \left(\frac{3\beta}{4}\frac{a}{R} + \frac{1}{4}\beta(1+\beta^2)\left(\frac{a}{R}\right)^3\right)(\boldsymbol{\delta} - \boldsymbol{dd})\right] \\ \boldsymbol{\omega}_1^{(1)} &= \frac{1}{2}\nabla \times \boldsymbol{v}_2|_{x=x_1} \\ &= -\frac{3}{4}\frac{b}{R^2}\boldsymbol{U}_2^{(0)} \times \boldsymbol{d} \\ \boldsymbol{S}_1^{(1)} &= \frac{20}{3}\pi\mu a^3(1 + \frac{a^2}{10}\nabla^2)\boldsymbol{e}_2|_{x=x_1} \\ &= \left(-\frac{5}{2}\frac{a^3}{R^2} + \frac{3}{2}\frac{a^5}{R^4}(1 + \frac{5}{3}\beta^2)\right)(\boldsymbol{dd} - \frac{1}{3}\boldsymbol{\delta})\boldsymbol{d} \cdot \boldsymbol{F}_2 \\ &\quad - \frac{1}{2}\frac{a^5}{R^4}(1 + \frac{5}{3}\beta^2)(\boldsymbol{F}_2\boldsymbol{d} + \boldsymbol{d}\boldsymbol{F}_2 - 2\boldsymbol{ddd} \cdot \boldsymbol{F}_2) . \end{aligned}$$

The algebraic reductions were obtained by inserting the appropriate expressions for $\mathcal{G}$ and its derivatives. Expressions for $\boldsymbol{U}_2^{(1)}$, $\boldsymbol{\omega}_2^{(1)}$, and $\boldsymbol{S}_2^{(1)}$ may be obtained from the preceding by switching a and b and the indices 1 and 2.

At the next (second) reflection, the fields $\boldsymbol{v}_{121}$ and $\boldsymbol{v}_{212}$ are expanded as

$$\begin{aligned} \boldsymbol{v}_{121} &= (\boldsymbol{S}_1^{(2)} \cdot \nabla) \cdot \frac{\mathcal{G}(\boldsymbol{x}-\boldsymbol{x}_1)}{(8\pi\mu)} + \cdots \\ \boldsymbol{v}_{212} &= (\boldsymbol{S}_2^{(2)} \cdot \nabla) \cdot \frac{\mathcal{G}(\boldsymbol{x}-\boldsymbol{x}_2)}{(8\pi\mu)} + \cdots , \end{aligned}$$

with motions and stresslets given by

$$\begin{aligned}
\boldsymbol{U}_1^{(2)} &= (1+\frac{a^2}{6}\nabla^2)\boldsymbol{v}_{12}|_{x=x_1} \\
&= \boldsymbol{U}_1^{(0)}\cdot\left[\left(-\frac{15}{4}\beta^3\left(\frac{a}{R}\right)^4\right)\boldsymbol{dd}+\left(O(R^{-6})(\boldsymbol{\delta}-\boldsymbol{dd})\right)\right] \\
\boldsymbol{\omega}_1^{(2)} &= \frac{1}{2}\nabla\times\boldsymbol{v}_{12}|_{x=x_1} = O(R^{-7}) \\
\boldsymbol{S}_1^{(2)} &= \frac{20}{3}\pi\mu a^3(1+\frac{a^2}{10}\nabla^2)\boldsymbol{e}_{12}|_{x=x_1} \\
&= \frac{25}{2}\beta^3\frac{a^6}{R^5}(\boldsymbol{dd}-\frac{1}{3}\boldsymbol{\delta})\boldsymbol{d}\cdot\boldsymbol{F}_1 \, .
\end{aligned}$$

The translational velocity contribution from the second reflection is $O(R^{-4})$ if the force on sphere 1 is directed along the axis, but is only $O(R^{-6})$ if the force is directed orthogonal to the axis. The second situation results in a weaker contribution, because the leading order term in $\boldsymbol{v}_{12}$ is a quadrupole field for that case. The angular velocity contribution from the second reflection is $O(R^{-7})$ instead of $O(R^{-5})$, because the leading order term in $\boldsymbol{v}_{12}$, a dipole field of cumulative strength of $O(R^{-4})$, is irrotational. As before, expressions for $\boldsymbol{U}_2^{(2)}$, $\boldsymbol{\omega}_2^{(2)}$, and $\boldsymbol{S}_2^{(2)}$ may be obtained from the analogous quantity for sphere 1 by switching a and b and the indices 1 and 2.

Since the final results are desired accurate to $O(R^{-5})$, the contributions from the third and fourth reflections are not needed. These will be $O(R^{-7})$ and $O(R^{-10})$, respectively. The results for $\boldsymbol{U}_1$ and $\boldsymbol{\omega}_1$ are obtained by adding the contributions from the reflections and are

$$\begin{aligned}
6\pi\mu a\boldsymbol{U}_1 &= -\boldsymbol{F}_1\cdot\left[\left(1-\frac{15}{4}\beta^3\left(\frac{a}{R}\right)^4\right)\boldsymbol{dd}+\left(1+O(R^{-6})\right)(\boldsymbol{\delta}-\boldsymbol{dd})\right] \\
&- \boldsymbol{F}_2\cdot\left[\left(\frac{3}{2}\frac{a}{R}-\frac{1}{2}(1+\beta^2)\left(\frac{a}{R}\right)^3\right)\boldsymbol{dd}\right. \\
&\qquad\left.+\left(\frac{3}{4}\frac{a}{R}+\frac{1}{4}(1+\beta^2)\left(\frac{a}{R}\right)^3\right)(\boldsymbol{\delta}-\boldsymbol{dd})\right] \\
6\pi\mu a^2\boldsymbol{\omega}_1 &= \boldsymbol{F}_1\times\boldsymbol{d}\left[O(R^{-7})\right]+\boldsymbol{F}_2\times\boldsymbol{d}\left[\frac{3}{4}\left(\frac{a}{R}\right)^2\right] \\
\boldsymbol{S}_1 &= \frac{25}{2}\beta^3\frac{a^6}{R^5}(\boldsymbol{dd}-\frac{1}{3}\boldsymbol{\delta})\boldsymbol{d}\cdot\boldsymbol{F}_1 \\
&+ \left(-\frac{5}{2}\frac{a^3}{R^2}+\frac{3}{2}\frac{a^5}{R^4}(1+\frac{5}{3}\beta^2)\right)(\boldsymbol{dd}-\frac{1}{3}\boldsymbol{\delta})\boldsymbol{d}\cdot\boldsymbol{F}_2 \\
&- \frac{1}{2}\frac{a^5}{R^4}(1+\frac{5}{3}\beta^2)(\boldsymbol{F}_2\boldsymbol{d}+\boldsymbol{d}\boldsymbol{F}_2-2\boldsymbol{ddd}\cdot\boldsymbol{F}_2)
\end{aligned}$$

and are consistent with the forms obtained for axisymmetric geometries, as discussed in the previous section. ◇

In the preceding example, the result for the case with forces along the line of centers may be inverted to obtain the solution of the corresponding resistance problem, to show that the results are consistent with the $O(R^{-4})$ calculation of Example 8.1 (see Exercise 8.5). For motions and forces perpendicular to the line of centers, we will also need the translational and rotational velocities of two force-free spheres subject to external torques (see Exercise 8.4). The two mobility problems can be combined to recover the resistance solution of Example 8.1 to $O(a/R)^5$. The important conclusion from these two examples is that the mobility solution can be obtained to higher order (R^{-5} *vs.* R^{-4}) with fewer reflections (two instead of four) than the corresponding resistance solution.

Example 8.4 Mobility Functions for Two Spherical Drops.
Consider two spherical *drops* centered at $\boldsymbol{x}_1$ and $\boldsymbol{x}_2$, and immersed in a fluid of viscosity μ. The sphere radii a and b, external forces $\boldsymbol{F}_1^e$ and $\boldsymbol{F}_2^e$, and $\beta = b/a$ are as in the preceding example. We keep things fairly general by allowing different drop viscosities, μ_1 and μ_2. Define viscosity ratios $\lambda_i = \mu_i/\mu$, $i = 1, 2$ and let $\Lambda_i = \lambda_i/(1+\lambda_i)$.

We generalize the preceding example to viscous drops by using the appropriate Faxén relations from Chapter 3,

$$\begin{aligned} \boldsymbol{U}_1 &= \left(1 + \frac{\Lambda_1 a^2 \nabla^2}{2(2+\Lambda_1)}\right) \boldsymbol{v}^\infty(\boldsymbol{x})|_{x=x_1} \\ \boldsymbol{S}_1 &= \frac{4}{3}(2+3\Lambda_1)\pi\mu a^3 \left(1 + \frac{\Lambda_1 a^2 \nabla^2}{2(2+3\Lambda_1)}\right) \boldsymbol{e}^\infty(\boldsymbol{x})|_{x=x_1} \ , \end{aligned}$$

in place of the ones for the rigid sphere. The other parts of the analysis are identical to those used in the preceding example, and the final result for the translational velocity on drop 1 may be written as

$$\begin{aligned} 6\pi\mu a \boldsymbol{U}_1 &= -\boldsymbol{F}_1 \cdot \left[\left(\frac{3}{2+\Lambda_1} - \frac{9\Lambda_2 + 6}{4}\beta^3 \left(\frac{a}{R}\right)^4\right) \boldsymbol{dd} \right. \\ &\qquad \left. + \left(\frac{3}{2+\Lambda_1} + O(R^{-6})\right)(\boldsymbol{\delta} - \boldsymbol{dd})\right] \\ &\quad - \boldsymbol{F}_2 \cdot \left[\left(\frac{3}{2}\frac{a}{R} - \frac{3}{2}\left(\frac{\Lambda_1}{2+\Lambda_1} + \frac{\Lambda_2\beta^2}{2+\Lambda_2}\right)\left(\frac{a}{R}\right)^3\right) \boldsymbol{dd} \right. \\ &\qquad \left. + \left(\frac{3}{4}\frac{a}{R} + \frac{3}{4}\left(\frac{\Lambda_1}{2+\Lambda_1} + \frac{\Lambda_2\beta^2}{2+\Lambda_2}\right)\left(\frac{a}{R}\right)^3\right)(\boldsymbol{\delta} - \boldsymbol{dd})\right] . \end{aligned}$$

◇

Example 8.5 Sedimentation of Two Spheroids in a Quiescent Fluid.
The hydrodynamic interaction between two prolate spheroids is of considerable interest as a model problem for suspensions consisting of elongated particles. Here, we generalize Example 8.3 (spheres) to prolate spheroids, following the treatment in Kim [44].

We take two spheroids centered at $\boldsymbol{x}_1$ and $\boldsymbol{x}_2$, and acted on by external forces $\boldsymbol{F}_1^e$ and $\boldsymbol{F}_2^e$. The zeroeth order solution for an isolated, translating prolate spheroid is expressed in the singularity form from Chapter 3:

$$\begin{aligned}
\boldsymbol{v}_1 &= \boldsymbol{F}_1^e \cdot \frac{1}{2k_1}\int_{-k_1}^{k_1}\left\{1+(k_1^2-\xi_1^2)\frac{(1-e_1^2)^2}{4e_1^2}\nabla^2\right\}\frac{\mathcal{G}(\boldsymbol{x}-\boldsymbol{\xi}_1)}{(8\pi\mu)}\,d\xi_1 \\
\boldsymbol{v}_2 &= \boldsymbol{F}_2^e \cdot \frac{1}{2k_2}\int_{-k_2}^{k_2}\left\{1+(k_2^2-\xi_2^2)\frac{(1-e_2^2)^2}{4e_2^2}\nabla^2\right\}\frac{\mathcal{G}(\boldsymbol{x}-\boldsymbol{\xi}_2)}{(8\pi\mu)}\,d\xi_2\ ,
\end{aligned}$$

with

$$6\pi\mu a\boldsymbol{U}_1^{(0)} = \boldsymbol{F}_1^e \cdot \left[(X^A)^{-1}\boldsymbol{d}_1\boldsymbol{d}_1 + (Y^A)^{-1}(\boldsymbol{\delta}-\boldsymbol{d}_1\boldsymbol{d}_1)\right]\ .$$

The axis of spheroid 1 is denoted by $\boldsymbol{d}_1$; $k_1 = ae_1$ is the focal parameter. The expression for $\boldsymbol{U}_2^{(0)}$ is quite similar and is obtained simply by switching labels 1 and 2.

The first reflection fields, $\boldsymbol{v}_{21}$ and $\boldsymbol{v}_{12}$, are represented to leading order by stresslets distributed over the spheroid axis. The explicit expression for the reflection at spheroid 1, $\boldsymbol{v}_{21}$, is

$$\boldsymbol{v}_{21} = (\boldsymbol{S}_1^{(1)}\cdot\nabla)\cdot\frac{3}{4k_1^3}\int_{-k_1}^{k_1}(k_1^2-\xi_1^2)\left\{1+(k_1^2-\xi_1^2)\frac{(1-e_1^2)^2}{8e_1^2}\nabla^2\right\}\frac{\mathcal{G}(\boldsymbol{x}-\boldsymbol{\xi}_1)}{(8\pi\mu)}\,d\xi_1+\cdots$$

with particle motions and stresslets obtained from the Faxén laws applied to the incident field, $\boldsymbol{v}_1$, *i.e.*,

$$\begin{aligned}
\boldsymbol{U}_1^{(1)} &= \frac{1}{2k_1}\int_{-k_1}^{k_1}\left\{1+(k_1^2-\xi_1^2)\frac{(1-e_1^2)^2}{4e_1^2}\nabla^2\right\}\boldsymbol{v}_2(\boldsymbol{\xi}_1)\,d\xi_1 \\
&= \boldsymbol{F}_2^e\cdot\int_{-k_1}^{k_1}\frac{d\xi_1}{2k_1}\int_{-k_2}^{k_2}\frac{d\xi_2}{2k_2}\left\{1+(k_1^2-\xi_1^2)\frac{(1-e_1^2)^2}{4e_1^2}\nabla_1^2\right. \\
&\qquad\left.+(k_2^2-\xi_2^2)\frac{(1-e_2^2)^2}{4e_2^2}\nabla_1^2\right\}\frac{\mathcal{G}(\boldsymbol{\xi}_1-\boldsymbol{\xi}_2)}{(8\pi\mu)} \\
\boldsymbol{\omega}_1^{(1)} &= \frac{3}{8k_1^3}\int_{-k_1}^{k_1}(k_1^2-\xi_1^2)\nabla\times\boldsymbol{v}_2(\boldsymbol{\xi}_1)\,d\xi_1 \\
&+ \frac{e_1^2}{(2-e_1^2)}\frac{3}{4k_1^3}\int_{-k_1}^{k_1}(k_1^2-\xi_1^2)\left\{1+(k_1^2-\xi_1^2)\frac{(1-e_1^2)^2}{8e_1^2}\nabla^2\right\} \\
&\qquad\times\boldsymbol{d}_1\times(\boldsymbol{e}_2(\boldsymbol{x}_1)\cdot\boldsymbol{d}_1)\,d\xi_1 \\
(\boldsymbol{S}_1^{(1)})_{ij} &= \frac{20}{3}\pi\mu a_1^3\left[X^M d_{ijkl}^{(0)} + Y^M d_{ijkl}^{(1)} + Z^M d_{ijkl}^{(2)}\right] \\
&\qquad\times\frac{3}{4k_1^3}\int_{-k_1}^{k_1}(k_1^2-\xi_1^2)\left\{1+(k_1^2-\xi_1^2)\frac{(1-e_1^2)^2}{8e_1^2}\nabla^2\right\}\boldsymbol{e}_2(\boldsymbol{\xi}_1)\,d\xi_1 \\
&+ 4\pi\mu a_1^3 Y^H(d_i\epsilon_{jkl}+d_j\epsilon_{ikl})d_l\frac{3}{8k_1^3}\int_{-k_1}^{k_1}(k_1^2-\xi_1^2)(\nabla\times\boldsymbol{v}_2(\boldsymbol{\xi}_1))_k\,d\xi_1\ .
\end{aligned}$$

Expressions for $\boldsymbol{U}_2^{(1)}$, $\boldsymbol{\omega}_2^{(1)}$, and $\boldsymbol{S}_2^{(1)}$ may be obtained from these preceding expressions by switching the spheroid labels 1 and 2.

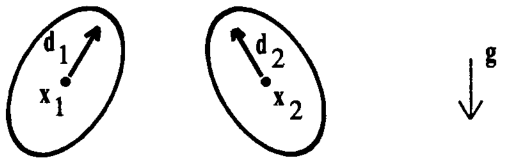

Figure 8.4: Two inclined prolate spheroids with axes in a common vertical plane.

The contributions from the next (second) reflection are obtained in exactly the same manner, with the incident field $\boldsymbol{v}_{12}$ in place of $\boldsymbol{v}_2$. While the final results are not as readily expressed in a form as compact as that encountered earlier for spheres, we may write a simple computer program to evaluate these integrals numerically, *e.g.*, by Gaussian quadratures, to obtain results for the mobility functions.

For example, consider two identical, inclined spheroids placed with their axes in a common vertical plane, as shown in Figure 8.4. Without hydrodynamic interaction, each spheroid would settle vertically, with a slight sideward drift induced by the anisotropy in the mobility tensor. However, each spheroid, being torque-free, must rotate in the common plane, with the angular velocity scaling with the vorticity of the Stokeslet field produced by the other (more precisely, an integrated weight of that vorticity field, as prescribed by the Faxén law). The change in orientation modifes the drift velocity so that the trajectory of the centroid is as shown in Figure 8.5. Note that both "single encounter" and periodic, meandering trajectories are possible. $\diamond$

8.4 Renormalization Theory

In Part II, we saw how bulk suspension properties, such as the effective viscosity, can be obtained from an analysis of the flow past a single particle. Naturally, those results were limited to dilute systems in which hydrodynamic interactions are negligible. We may now use our knowledge of pair interactions to obtain the first corrections, and it is reasonable to expect that the solution takes the form of a virial expansion in the volume fraction c. For example, the effective viscosity of a suspension of rigid spheres should be of the form

$$\frac{\mu^{\text{eff}}}{\mu} = 1 + \frac{5}{2}c + Bc^2 + \dots ,$$

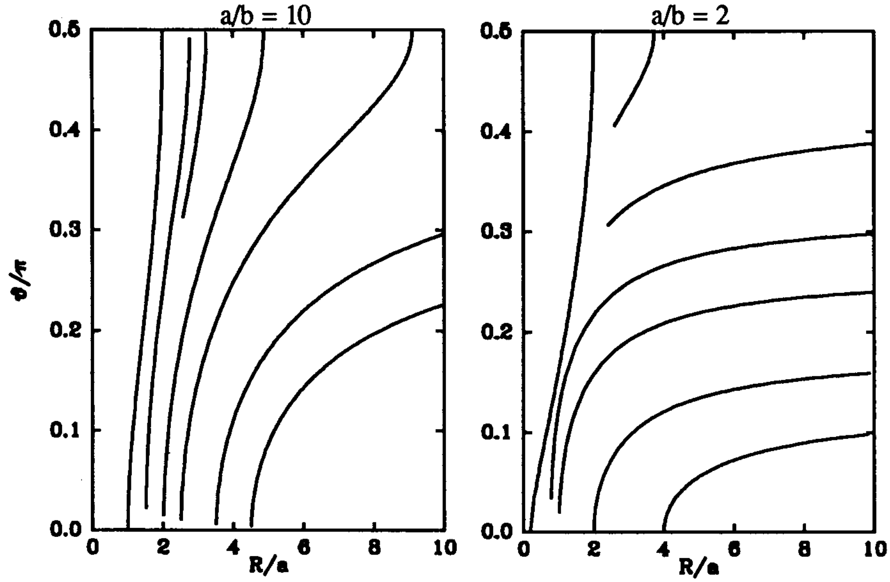

Figure 8.5: Spheroid (centroid) trajectories.

with the precise value of B depending on the details of the two-particle problem. Indeed, going through the steps described in Chapter 2, we have

$$\sigma^{\text{eff}} = \sigma^{\text{fluid}} + \sigma^{\text{particle}} ,$$

with the particle contribution to the bulk stress given by an ensemble average of the stresslet,

$$\sigma^{\text{particle}} = n < \boldsymbol{S} > .$$

Following the usual procedure of statistical physics, we would expect a result in terms of the configurational integral,

$$< \boldsymbol{S} >= \boldsymbol{S}_0 + \int_{|x_2 - x_1 \geq 2a|} P(\boldsymbol{x}_2|\boldsymbol{x}_1)(\boldsymbol{S}_{12} - \boldsymbol{S}_0)\, dV(\boldsymbol{x}_2) + O(c^2) .$$

Here, $\boldsymbol{S}_0 = \frac{20}{3}\pi\mu a^3 \boldsymbol{E}^\infty$ is the single-sphere result for the stresslet; $\boldsymbol{S}_{12} - \boldsymbol{S}_0$ is the "excess" stresslet on sphere 1 due to hydrodynamic interactions with another sphere at $\boldsymbol{x}_2$. This pair contribution to the bulk stress is obtained by integration over all allowed positions of sphere 2, with contributions weighted according to the conditional pair probability $P(\boldsymbol{x}_2|\boldsymbol{x}_1)$. But this simple approach encounters difficulties in the problems of microhydrodynamics, because the interactions between the particles are too strong.

For a dilute suspension, we expect $P(\boldsymbol{x}_2|\boldsymbol{x}_1) \sim n$, the number density, as $|\boldsymbol{x}_2 - \boldsymbol{x}_1| \to \infty$. While this leads to the expected scaling of $O(c^2)$, the excess

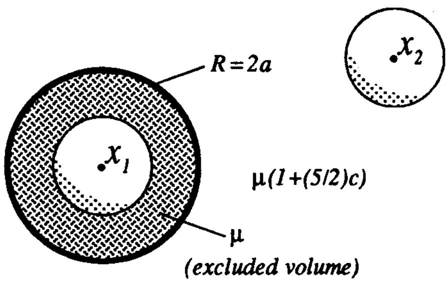

Figure 8.6: The effective medium in the renormalized formulation.

stresslet, $S_{12} - S_0$ decays as R^{-3} so that the configurational integral is of the form

$$\int_{2a}^{R^\infty} R^{-3} R^2 \, dR \,,$$

which is nonconvergent as $R^\infty \to \infty$.

The resolution of this paradox is given in a number of important papers in the development of suspension rheology [2, 29, 36, 57]. The successive limits of large R^∞ and small c do not commute. Indeed, fixing c first at a small value we see that there is a new length scale $a/c^{1/3}$, and in a volume much larger than these dimensions there will be many spheres. Thus for R^∞ much greater than this length, the pair interactions S_{12} occur in an effective medium quite different from the pure solvent. In fact, for the purposes of the $O(c^2)$ problem, we may approximate the effective medium as a Newtonian fluid with the Einstein viscosity. In general, nonconvergent interactions indicate that the limiting processes mentioned above do not commute and that screening in an effective medium should be taken into consideration [29].

To pursue this in a more concrete setting, we average the governing balance equation over all realizations containing a sphere centered at $\boldsymbol{x}_1$, leaving the conditionally averaged equation,

$$\begin{aligned} -\nabla < p > (\boldsymbol{x}|\boldsymbol{x}_1) + \mu \nabla^2 < \boldsymbol{v} > (\boldsymbol{x}|\boldsymbol{x}_1) \\ = \int_{R \geq 2a} P(\boldsymbol{x}_2|\boldsymbol{x}_1) \oint_{|\xi - x_2| = a} < \boldsymbol{\sigma} > (\boldsymbol{\xi}|\boldsymbol{x}_1, \boldsymbol{x}_2) \cdot \boldsymbol{n}(\boldsymbol{\xi}) \delta(\boldsymbol{x} - \boldsymbol{\xi}) \, dS(\boldsymbol{\xi}) \ . \end{aligned} \quad (8.1)$$

The physical meaning of this equation is that in all realizations with a sphere at $\boldsymbol{x}_1$, the fluid satisfies the inhomogeneous Stokes equations, with the body forces given exactly by the surface tractions on the other spheres. The latter effect is of course weighted by the conditional probability of a second sphere configured at $\boldsymbol{x}_2$. If we make what appears to be a reasonable approximation, replace $< \boldsymbol{\sigma} > (\boldsymbol{\xi}|\boldsymbol{x}_1, \boldsymbol{x}_2)$ with that of two spheres in the pure Newtonian solvent and a small relative error of $O(c)$, then the error is made and the noncovergent integrals arise. As mentioned above, this approximation is not uniformly valid in $V(\boldsymbol{x}_2)$. However, if we approximate $<\boldsymbol{\sigma}>(\boldsymbol{\xi}|\boldsymbol{x}_1,\boldsymbol{x}_2)$ with that of two spheres in the Einstein medium with viscosity $\mu(1+\frac{5}{2}c)$, the error is still of $O(c)$, but is now uniformly valid throughout $V(\boldsymbol{x}_2)$. Indeed, borrowing from cell and self-consistent field theories, we may use the Einstein viscosity only beyond a certain value of R. The exact location of this viscosity jump does not alter the final result for the virial expansion, but does shift favorably the relative contributions of the analytical over the numerical portions in the final expression for the viscosity [43].

Hinch, in his original work [29], places the viscosity jump at $R=2a$, or the excluded volume radius, and the renormalized formulation is

$$\begin{aligned}
&-\nabla <p>(\boldsymbol{x}|\boldsymbol{x}_1)+\mu\nabla^2 <\boldsymbol{v}>(\boldsymbol{x}|\boldsymbol{x}_1)\\
&+\int_{R\geq 2a}\frac{5}{2}\mu c\nabla_2^2 <\boldsymbol{v}>(\boldsymbol{x}_2|\boldsymbol{x}_1)\delta(\boldsymbol{x}-\boldsymbol{x}_2)\,dV(\boldsymbol{x}_2)\\
&+\left(\oint_{R=2a}-\oint_{\infty}\right)5\mu c <\boldsymbol{e}>(\boldsymbol{x}_2|\boldsymbol{x}_1)\cdot\boldsymbol{n}_2\delta(\boldsymbol{x}-\boldsymbol{x}_2)\,dS(\boldsymbol{x}_2)\\
&=\int_{R\geq 2a}\left\{P(\boldsymbol{x}_2|\boldsymbol{x}_1)\oint_{|\xi-x_2|=a}<\boldsymbol{\sigma}>(\boldsymbol{\xi}|\boldsymbol{x}_1,\boldsymbol{x}_2)\cdot\boldsymbol{n}(\boldsymbol{\xi})\delta(\boldsymbol{x}-\boldsymbol{\xi})\,dS(\boldsymbol{\xi})\right.\\
&\qquad\left.-5\mu c <\boldsymbol{e}>(\boldsymbol{x}_2|\boldsymbol{x}_1)\cdot\nabla_2\delta(\boldsymbol{x}-\boldsymbol{x}_2)\right\}\,dV(\boldsymbol{x}_2)\,. \qquad (8.2)
\end{aligned}$$

Using the properties of the Dirac delta function, we see that the left-hand side of this equation has a viscosity jump at $R=2a$, from the pure solvent value to the Einstein viscosity. Comparing Equations 8.1 and 8.2, as long as the exact conditionally averaged field variables are retained, the two equations are identical. The new terms appearing in the renormalized equation cancel exactly, by an application of the Green's identity and the divergence theorem. However, the renormalized equation is the one in which the effect of the second test sphere (the inhomogeneous terms on the right-hand side) can be uniformly truncated with respect to small c.

The stresslet on sphere 1 for Equation 8.2 can be written directly using the Faxén relation, and ultimately leads to the following expression for the bulk stress:

$$\begin{aligned}
\boldsymbol{\sigma}(\boldsymbol{x}) &= -p(\boldsymbol{x})\boldsymbol{\delta}+2\mu(1+\frac{5}{2}c)\boldsymbol{e}(\boldsymbol{x})+\frac{515}{64}\mu c^2\boldsymbol{e}(\boldsymbol{x})\\
&+ P(\boldsymbol{x})\int_{R\geq 2a}\{P(\boldsymbol{x}_2|\boldsymbol{x}_1)(\boldsymbol{S}_{12}(\boldsymbol{x}|\boldsymbol{x}_2)-\boldsymbol{S}_0)\\
&\qquad -5\mu c\boldsymbol{E}^D\left((\boldsymbol{x},\boldsymbol{x}_2,\boldsymbol{e}+\boldsymbol{E}^{\infty})\right)\Big\}\,dV(\boldsymbol{x}_2)\,. \qquad (8.3)
\end{aligned}$$

The term $\frac{515}{64}\mu c^2\boldsymbol{e}(\boldsymbol{x})$ comes from the viscosity jump, *i.e.*, the stresslet on an isolated sphere in a pure rate-of-strain field in a fluid medium with a viscosity jump at $R=2a$.

The distribution of dipoles subtracted on the RHS of Equation 8.2 originated as part of the renormalization procedure. Thus the original nonconvergent integrand, $(\boldsymbol{S}_{12}(\boldsymbol{x}|\boldsymbol{x}_2)-\boldsymbol{S}_0)$, has been modified by a disturbance rate-of-strain field $\boldsymbol{E}^D(\boldsymbol{x},\boldsymbol{x}_2,\boldsymbol{e}+\boldsymbol{E}^D)$. The arguments denote that this is the extra rate-of-strain due to the presence of a second sphere at $\boldsymbol{x}_2$ and that the sphere at $\boldsymbol{x}_2$

is immersed in an ambient flow with the rate of strain $\boldsymbol{e} + \boldsymbol{E}^D$. (To get the usual notation in this book, map $\boldsymbol{e} \rightarrow \boldsymbol{E}^\infty$ and $\boldsymbol{E}^D \rightarrow \boldsymbol{e}_1$, the rate-of-strain field of the first reflection from sphere 1.) The reader should verify that the definition for $\boldsymbol{E}^D((\boldsymbol{x}, \boldsymbol{x}_2, \boldsymbol{e} + \boldsymbol{E}^D))$ is precisely that required for the zeroeth, first and second reflection contributions to the stresslet on sphere 1, and thus the modified integrand now decays as $O(R^{-8})$.

A numerical solution of the two-sphere problem is necessary to obtain the excess stresslet to complete the solution [2, 45, 69]. It should be noted that the pair probability, $P(\boldsymbol{x}_2|\boldsymbol{x}_1)$, for the flowing suspension cannot be set arbitrarily, but must be obtained by solving the pair conservation equation:

$$\frac{\partial}{\partial t} P(\boldsymbol{x}_2|\boldsymbol{x}_1) + \nabla_2 \cdot ((\boldsymbol{U}_2 - \boldsymbol{U}_1) P(\boldsymbol{x}_2|\boldsymbol{x}_1)) = 0 \ . \tag{8.4}$$

For pure rate-of-strain flow, $\boldsymbol{U}_2 - \boldsymbol{U}_1$ can be written in terms of two mobility functions A and B (see Chapter 11) as

$$\boldsymbol{U}_2 - \boldsymbol{U}_1 = \boldsymbol{E}^\infty \cdot (\boldsymbol{x}_2 - \boldsymbol{x}_1) - [A(R)\boldsymbol{dd} + B(R)(\boldsymbol{\delta} - \boldsymbol{dd})] \cdot \boldsymbol{E}^\infty \cdot (\boldsymbol{x}_2 - \boldsymbol{x}_1) \ .$$

With the condition that $P(\boldsymbol{x}_2|\boldsymbol{x}_1) \rightarrow n$ as $R \rightarrow \infty$, Equation 8.4 has the exact solution,

$$P(\boldsymbol{x}_2|\boldsymbol{x}_1) = \frac{n}{1-A} \exp\left\{ \int_R^\infty \frac{3(B(\rho) - A(\rho))}{\rho(1 - A(\rho))} \, d\rho \right\} \ .$$

Numerical integration of the last term in Equation 8.3 is all that remains in the calculation of the $O(C^2)$ coefficient of the viscosity.

Equation 8.4 cannot be solved for simple shear flows, because the spheres form doublets (see Chapter 11) whose history cannot be traced to conditions at infinity. Higher order effects, such as Brownian diffusion, must be included [14, 15]. For pure rate-of-strain fields, the conservation equation can be solved and $P(\boldsymbol{x}_1|\boldsymbol{x}_2)$ can be expressed in terms of the two-sphere mobility functions x^g and y^g, and the final result for the effective viscosity is[2]

$$\frac{\mu^{\text{eff}}}{\mu} = 1 + \frac{5}{2} c + 6.95 c^2 + \dots \ .$$

8.5 Multipole Expansions for Two Spheres

The method of reflections as outlined in the previous section is a general solution strategy that generates a series solution suitable for determining interactions between particles of arbitrary shape, as long as they are far apart. The method is viable under these conditions because the algebraic manipulations for the first few terms in the series are quite simple. As the particles approach each other, the number of terms required in this series increases. The effort required to

[2] In 1972, accurate results for the stresslets of the two-sphere problem were not available. The often-quoted value 7.6 for the $O(c^2)$ coefficient given in the original work [2] was obtained from a rough interpolation that overestimated the contributions from the sphere-sphere interactions.

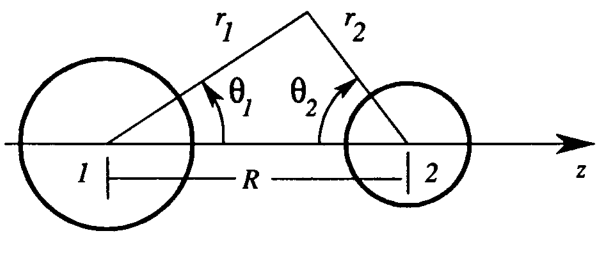

Figure 8.7: The two-sphere geometry

obtain the higher-order terms is prohibitive and the method becomes less attractive. However, for the special case of two spheres, we can still obtain series solutions by the judicious use of transformation formulas relating Lamb's solution expanded with respect to two different origins. The method was developed by Jeffrey and Onishi [38], and the discussion in this section borrows heavily from their work.

In a nutshell, we borrow the form of the velocity representation from the method of reflections and expand the disturbance field about the two sphere centers, but now the boundary conditions at each sphere are set simultaneously. Of course, the disturbance field from the other sphere presents some problems since those fields are cast in terms of a coordinate system based on a different origin (located at the other sphere's center). However, spherical harmonics based at one origin can be recast in terms of those expanded about another origin, by the so-called addition theorems [30], and since our velocity fields are closely related to, and in fact derived from spherical harmonics, we find that the disturbance field about one sphere may be written in terms of velocity fields expanded about the other.

The two-sphere geometry is shown in Figure 8.7 The spheres are centered at $\boldsymbol{x}_1$ and $\boldsymbol{x}_2$, and their radii are denoted by $a_1 = a$ and $a_2 = b$. Spherical polar coordinates (r_1, θ_1, ϕ) about the origin $\boldsymbol{x}_1$ are defined in the usual fashion, with $\boldsymbol{d} = (\boldsymbol{x}_2 - \boldsymbol{x}_1)/R$ as the polar $(z-)$ axis. For (r_2, θ_2, ϕ) we use a *left-handed* system, with $\boldsymbol{e}_r^{(2)} \times \boldsymbol{e}_\theta^{(2)} = -\boldsymbol{e}_\phi$, to simplify the form taken by addition theorem for the spherical harmonics. Based on Hobson [30], we write the addition theorem as

$$\left(\frac{a_\alpha}{r_\alpha}\right)^{n+1} Y_{mn}(\theta_\alpha, \phi) = \left(\frac{a_\alpha}{R}\right)^{n+1} \sum_{s=m}^{\infty} \begin{pmatrix} n+s \\ s+m \end{pmatrix} \left(\frac{r_{3-\alpha}}{R}\right)^s Y_{ms}(\theta_{3-\alpha}, \phi) \;, \quad (8.5)$$

with $\alpha = 1, 2$, depending on whether we wish to expand harmonics based on $\boldsymbol{x}_1$ in terms of those at $\boldsymbol{x}_2$ or *vice-versa.* A right-handed system can be defined at $\boldsymbol{x}_2$, *i.e.*, by letting $\theta_2 \to \pi - \theta_2$, but this will introduce a factor of -1 in a number of places in the following discussion.

The pressure and velocity fields are written as a linear combination of two sets of Lamb's solution (one for each sphere center):

$$p = p^{(1)} + p^{(2)} , \qquad \boldsymbol{v} = \boldsymbol{v}^{(1)} + \boldsymbol{v}^{(2)} ,$$

with

$$p^{(\alpha)} = \frac{\mu}{a_\alpha} \sum_{m=0}^{\infty} \sum_{n=m}^{\infty} A_{mn}^{(\alpha)} \left(\frac{a_\alpha}{r_\alpha}\right)^{n+1} Y_{mn}(\theta_\alpha, \phi)$$

$$\begin{aligned} \boldsymbol{v}^{(\alpha)} = & \sum_{m=0}^{\infty} \sum_{n=m}^{\infty} \left\{ \frac{-(n-2)r_\alpha^2}{2n(2n-1)a_\alpha} \nabla \left[A_{mn}^{(\alpha)} \left(\frac{a_\alpha}{r_\alpha}\right)^{n+1} Y_{mn}(\theta_\alpha, \phi) \right] \right. \\ & + \frac{(n+1)\boldsymbol{r}_\alpha}{n(2n-1)a_\alpha} A_{mn}^{(\alpha)} \left(\frac{a_\alpha}{r_\alpha}\right)^{n+1} Y_{mn}(\theta_\alpha, \phi) \\ & + a_\alpha \nabla \left[B_{mn}^{(\alpha)} \left(\frac{a_\alpha}{r_\alpha}\right)^{n+1} Y_{mn}(\theta_\alpha, \phi) \right] \\ & \left. + \nabla \times \left[C_{mn}^{(\alpha)} \left(\frac{a_\alpha}{r_\alpha}\right)^{n+1} Y_{mn}(\theta_\alpha, \phi) \right] \right\} . \end{aligned}$$

The existence of such representations can be argued by appealing to the form taken by the usual Taylor series operation with the surface variable of the integral representation for the two-sphere velocity field. Note that the equations have been scaled so that the coefficients $A_{mn}^{(\alpha)}$, $B_{mn}^{(\alpha)}$, and $C_{mn}^{(\alpha)}$ have dimensions of velocities.

On the sphere surfaces, we take the known boundary velocity $\boldsymbol{V}^{(\alpha)}(\theta_\alpha, \phi)$ and set the radial velocity, surface divergence, and surface vorticity as explained in Chapter 4. For the sake of argument, we assume these known quantities can be written as

$$\begin{aligned} \boldsymbol{v} \cdot \boldsymbol{e}_r^{(\alpha)} &= \boldsymbol{V}^{(\alpha)} \cdot \boldsymbol{e}_r^{(\alpha)} &= \sum_{m=0}^{\infty} \sum_{n=m}^{\infty} R_{mn}^{(\alpha)} Y_{mn}(\theta_\alpha, \phi) \\ \boldsymbol{r}_\alpha \cdot \nabla(\boldsymbol{v} \cdot \boldsymbol{e}_r^{(\alpha)}) &= -r_\alpha \nabla \cdot \boldsymbol{V}^{(\alpha)} \cdot \boldsymbol{e}_r^{(\alpha)} &= \sum_{m=0}^{\infty} \sum_{n=m}^{\infty} D_{mn}^{(\alpha)} Y_{mn}(\theta_\alpha, \phi) \\ \boldsymbol{r}_\alpha \cdot \nabla \times \boldsymbol{v} &= \boldsymbol{r}_\alpha \nabla \times \boldsymbol{V}^{(\alpha)} &= \sum_{m=0}^{\infty} \sum_{n=m}^{\infty} \omega_{mn}^{(\alpha)} Y_{mn}(\theta_\alpha, \phi) . \end{aligned}$$

As in Chapter 4, the boundary conditions yield three sets of equations, after collection of terms corresponding to each spherical harmonic. The new wrinkle comes from terms that originate from the other sphere, which must be recast in the more usable form by applying the addition theorem, Equation 8.5. Because we are dealing with vector quantities, we will also need the following geometric relations:

$$\begin{aligned} \boldsymbol{e}_r^{(\alpha)} &= (r_{3-\alpha} - R\cos\theta_{3-\alpha})\boldsymbol{e}_r^{(3-\alpha)} + R\sin\theta_{3-\alpha}\boldsymbol{e}_\theta^{(3-\alpha)} \\ r_\alpha^2 &= R^2 + r_{3-\alpha}^2 - 2Rr_{3-\alpha}\cos\theta_{3-\alpha} . \end{aligned}$$

The following relations are obtained after some considerable algebra:

$$\begin{aligned}
&(n+1)(2n+1)B_{mn}^{(\alpha)} - \frac{1}{2}(n+1)A_{mn}^{(\alpha)} + \frac{n}{2n+3}\sum_{s=m}^{\infty}\begin{pmatrix} n+s \\ n+m \end{pmatrix} A_{ms}^{(3-\alpha)} t_\alpha^{n+1} t_{3-\alpha}^{s} \\
&= D_{mn}^{(\alpha)} - (n-1)R_{mn}^{(\alpha)}
\end{aligned} \tag{8.6}$$

$$\begin{aligned}
&\frac{n+1}{2n-1}A_{mn}^{(\alpha)} + \sum_{s=m}^{\infty}\begin{pmatrix} n+s \\ n+m \end{pmatrix} t_\alpha^{n-1} t_{3-\alpha}^{s} \Big[(-1)^\alpha m(2n+1)iC_{ms}^{(3-\alpha)}t_{3-\alpha} \\
&\qquad + n(2n+1)B_{ms}^{(3-\alpha)}t_{3-\alpha}^2 \\
&\qquad + \left(\frac{n+1}{2n-1}\right)\frac{ns(n+s-2ns-2)-m^2(2ns-4s-4n+2)}{2s(2s-1)(n+s)}A_{ms}^{(3-\alpha)} \\
&\qquad + \frac{n}{2}A_{ms}^{(3-\alpha)}t_\alpha^2\Big] \\
&= D_{mn}^{(\alpha)} + (n+2)R_{mn}^{(\alpha)}
\end{aligned} \tag{8.7}$$

$$\begin{aligned}
&n(n+1)C_{mn}^{(\alpha)} + \sum_{s=m}^{\infty}\begin{pmatrix} n+s \\ n+m \end{pmatrix} t_\alpha^{n} t_{3-\alpha}^{s}\left[-nsC_{ms}^{(3-\alpha)}t_{3-\alpha} + (-1)^\alpha\frac{m}{s}iA_{ms}^{(3-\alpha)}\right] \\
&= \omega_{mn}^{(\alpha)} ,
\end{aligned} \tag{8.8}$$

where $t_\alpha = a_\alpha/R$. These equations may be solved by a number of different methods, but we shall focus our attention on getting the final solution in the form of a series in R^{-1}.

8.5.1 Translations Along the Axis

The problem of motions along the sphere-sphere axis are decomposed into two subproblems; the first involving two spheres approaching each other with equal velocities and the second involving two spheres translating together at the same velocity. We may then exploit certain symmetries in these two problems to reduce the work involved.

Resistance Functions for Two Approaching Spheres

In the first problem, we set $\boldsymbol{V}_1 = \boldsymbol{U}_1 = U\boldsymbol{d}$, $\boldsymbol{V}_2 = \boldsymbol{U}_2 = -U\boldsymbol{d}$, so that

$$R_{mn}^{(\alpha)} = U\delta_{m0}\delta_{n1} , \qquad D_{mn}^{(\alpha)} = \omega_{mn}^{(\alpha)} = 0 .$$

Since the problem is axisymmetric, only terms corresponding to $m = 0$ are relevant, and since we are not dealing with a "swirling" flow, we do not need $C_{0n}^{(\alpha)}$. We expand $A_{0n}^{(\alpha)}$ and $B_{0n}^{(\alpha)}$ as a power series in R^{-1}, *i.e.*,

$$\begin{aligned}
A_{0n}^{(\alpha)} &= \frac{3}{2}U\sum_{p=0}^{\infty}\sum_{q=0}^{\infty} A_{npq}^{(\alpha)} t_\alpha^p t_{3-\alpha}^q \\
B_{0n}^{(\alpha)} &= \frac{3}{4}U\sum_{p=0}^{\infty}\sum_{q=0}^{\infty} \frac{1}{2n+1} B_{npq}^{(\alpha)} t_\alpha^p t_{3-\alpha}^q .
\end{aligned}$$

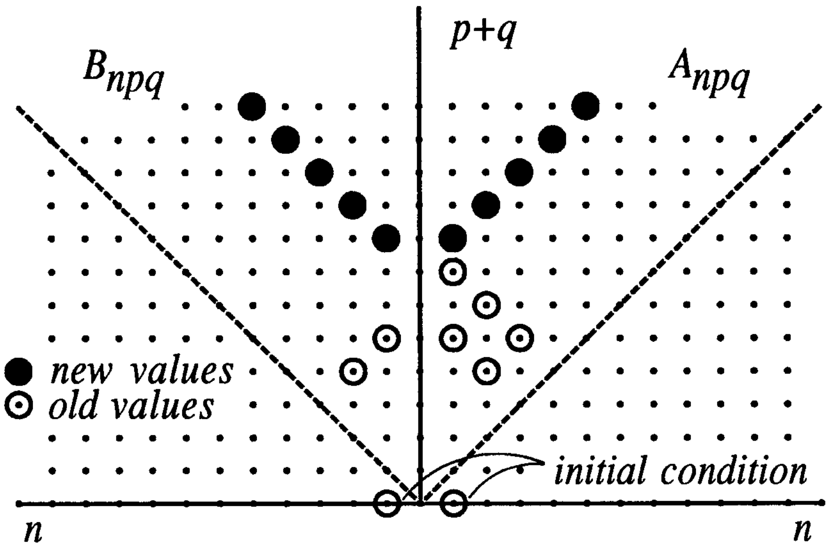

Figure 8.8: The recursion relations for A_{npq} and B_{npq}.

(We have made use of the final result to redefine the expansion parameters so as to simplify the initial conditions and recursion relations.)

We insert these expansions into Equations 8.6 and 8.7 to obtain the recursion relations,

$$A_{n00} = B_{n00} = \delta_{1n}$$

$$\begin{aligned} A_{npq} &= \sum_{s=1}^{q} \binom{n+s}{n} \left[\frac{n(2n+1)(2ns-n-s+2)}{2(n+1)(2s-1)(n+s)} A_{s(q-s)(p-n+1)} \right. \\ &\quad \left. - \frac{n(2n-1)}{2(n+1)} A_{s(q-s)(p-n-1)} - \frac{n(2n-1)(2n+1)}{2(n+1)(2s+1)} B_{s(q-s-2)(p-n+1)} \right] \end{aligned}$$

$$B_{npq} = A_{npq} - \frac{2n}{(n+1)(2n+3)} \sum_{s=1}^{q} \binom{n+s}{n} A_{s(q-s)(p-n-1)} \ .$$

The label α has been dropped since the coefficients are identical for the two spheres. (This can be shown explicitly from the recursion relations and is ultimately due to the symmetry in the problem.) The operation of the recursion relation is shown schematically in Figure 8.8. The essential advantage of this approach over the method of reflections is that the recursion relations can be easily programmed into a computer, and many terms can be generated.

The force on sphere α is given by

$$\boldsymbol{F}_\alpha = 4\pi\mu a_\alpha (-1)^\alpha A_{01}^{(\alpha)} \boldsymbol{d} \ .$$

With both spheres 1 and 2 moving, the force on sphere 1 is given by

$$X_{11}^A - X_{12}^A = 6\pi a \sum_{p=0}^{\infty}\sum_{q=0}^{\infty} A_{1pq} t_1^p t_2^q \ .$$

Resistance Functions for Two Spheres Moving in Tandem

In the second problem, we set $\boldsymbol{V}_1 = \boldsymbol{V}_2 = U\boldsymbol{d}$, and here we find

$$R_{mn}^{(\alpha)} = (-1)^{3-\alpha} U \delta_{m0}\delta_{n1} \ , \qquad D_{mn}^{(\alpha)} = \omega_{mn}^{(\alpha)} = 0 \ .$$

We repeat the procedure just used for spheres approaching each other and obtain a similar set of recursion relations. In fact, an examination of the new recursion relations reveals that it may be transformed to the old recursion relations if A_{npq} and B_{npq} are replaced everywhere by $(-1)^{n+p+q+\alpha}A_{npq}$ and $(-1)^{n+p+q+\alpha}B_{npq}$. This, of course, was the reason why the translation problem was decomposed into two subproblems in the first place. Since the spheres are moving in tandem, the force on sphere 1 is now given by

$$X_{11}^A + X_{12}^A = 6\pi a \sum_{p=0}^{\infty}\sum_{q=0}^{\infty} (-1)^{p+q} A_{1pq} t_1^p t_2^q \ ,$$

where A_{1pq} is that obtained in the previous problem.

Since we know the sum and difference of X_{11}^A and X_{12}^A, we can derive explicit expressions for both. We find that X_{11}^A is a series in even powers of R^{-1}, whereas X_{12}^A is a series in odd powers of R^{-1}. The first few terms of the final result are tabulated in Chapter 11.

Mobility Functions for Two Approaching Spheres

In the mobility problems, $\boldsymbol{F}_1$ and $\boldsymbol{F}_2$ are known and $\boldsymbol{U}_1$ and $\boldsymbol{U}_2$ are to be determined. Of course, having obtained the resistance functions, we could simply invert the resistance matrix. However, it is also possible to obtain the mobility functions directly, with a minor modification of the recursion scheme. First, assume that the forces are in opposite directions such that the scaled forces satisfy

$$(6\pi\mu a_1)^{-1}\boldsymbol{F}_1 = -(6\pi\mu a_2)^{-1}\boldsymbol{F}_2 = U\boldsymbol{d} \ .$$

The physical significance of U is that it is the approach velocity that each sphere, when isolated, would experience when subject to these forces, as a consequence of Stokes' law. Our task is to determine the actual velocities, $\boldsymbol{U}_1$ and $\boldsymbol{U}_2$, which differ from the widely separated value because of hydrodynamic interactions. We shall write these unknown velocities as

$$\boldsymbol{U}_1 = U^{(1)}\boldsymbol{d} \ , \qquad \boldsymbol{U}_2 = -U^{(2)}\boldsymbol{d} \ .$$

Since $\boldsymbol{\omega}_1 = \boldsymbol{\omega}_2 = \boldsymbol{0}$ we may set

$$R_{mn}^{(\alpha)} = U_\alpha \delta_{m0}\delta_{n1} \ , \qquad D_{mn}^{(\alpha)} = \omega_{mn}^{(\alpha)} = 0 \ ,$$

and drop the $C_{0n}^{(\alpha)}$ terms. We expand $A_{0n}^{(\alpha)}$, $B_{0n}^{(\alpha)}$, and $U^{(\alpha)}$ as

$$\begin{aligned} A_{0n}^{(\alpha)} &= \frac{3}{2}U\sum_{p=0}^{\infty}\sum_{q=0}^{\infty} A_{npq}t_{\alpha}^{p}t_{3-\alpha}^{q} \\ B_{0n}^{(\alpha)} &= \frac{3}{4}U\sum_{p=0}^{\infty}\sum_{q=0}^{\infty} \frac{1}{2n+1}B_{npq}t_{\alpha}^{p}t_{3-\alpha}^{q} \\ U^{(\alpha)} &= U\sum_{p=0}^{\infty}\sum_{q=0}^{\infty} U_{pq}t_{\alpha}^{p}t_{3-\alpha}^{q} , \end{aligned}$$

and, as before, the two spheres have the same coefficients and the label α is not needed.

Since the force is known, the initial conditions of the recursion relations now read

$$A_{1pq} = \delta_{0p}\delta_{0q} .$$

For $n = 1$, Equation 8.6 provides an equation for U_{pq},

$$U_{pq} = -\sum_{s=1}^{q}(s+1)\left[\frac{3A_{s(q-s)p}}{4(2s-1)} - \frac{1}{4}A_{s(q-s)(p-2)} - \frac{3B_{s(q-s-2)p}}{4(2s+1)}\right] ,$$

while for $n > 1$, it is a recursion relation for A_{npq},

$$\begin{aligned} A_{npq} &= \sum_{s=1}^{q}\binom{n+s}{n}\left[\frac{n(2n+1)(2ns-n-s+2)}{2(n+1)(2s-1)(n+s)}A_{s(q-s)(p-n+1)}\right. \\ &\quad \left. -\frac{n(2n-1)}{2(n+1)}A_{s(q-s)(p-n-1)} - \frac{n(2n-1)(2n+1)}{2(n+1)(2s+1)}B_{s(q-s-2)(p-n+1)}\right] . \end{aligned}$$

Equation 8.7 remains valid for all $n \geq 1$ and provides a recursion relation for B_{npq}.

$$B_{npq} = A_{npq} - \frac{2n}{(n+1)(2n+3)}\sum_{s=1}^{q}\binom{n+s}{n}A_{s(q-s)(p-n-1)} .$$

With the assumed hydrodynamic forces acting on spheres 1 and 2, the translation velocity of sphere 1 provides the relation,

$$6\pi a x_{11}^{a} - 6\pi b x_{12}^{a} = \sum_{p=0}^{\infty}\sum_{q=0}^{\infty} U_{pq}t_1^p t_2^q .$$

Mobility Functions for Forces in the Same Direction

In the second mobility problem, we set

$$(6\pi\mu a_1)^{-1}\boldsymbol{F}_1 = (6\pi\mu a_2)^{-1}\boldsymbol{F}_2 = U\boldsymbol{d} ,$$

and ultimately we find that the coefficients are given by $(-1)^{p+q}U_{pq}$, where U_{pq} is that obtained in the first problem:

$$6\pi a x_{11}^{a} + 6\pi b x_{12}^{a} = \sum_{p=0}^{\infty}\sum_{q=0}^{\infty}(-1)^{p+q}U_{pq}t_1^p t_2^q .$$

As was the case in the resistance problem, the $1-1$ function, x^a_{11}, is a series in even powers of R^{-1} while the $1-2$ function, x^a_{12}, is a series in odd powers of R^{-1}. The first few terms of the final result are tabulated in Chapter 11.

8.6 Electrophoresis of Particles with Thin Double Layers

8.6.1 Hydrodynamic Interaction Between Spheres

In Chapter 5, we considered electrophoresis of particle with thin electrical double layers and showed that the mobility was independent of particle shape. We now consider the role of hydrodynamic interactions for two widely separated particles. The method of reflection analysis shown here follows closely that of Chen and Keh [6], who considered the interaction between two spherical colloidal particles.

Consider two spheres with surface (zeta) potentials ζ_1 and ζ_2 undergoing electrophoresis in response to an applied electric field $\boldsymbol{E}^\infty$. In all other respects, the two-sphere geometry is as in earlier sections of this chapter. The governing equations for the electric field, electrostatic potential, the hydrodynamic variables are

$$\begin{aligned}
\nabla\cdot\boldsymbol{E} &= -\nabla^2\psi = 0\\
\hat{\boldsymbol{n}}\cdot\boldsymbol{E} &= 0 \quad \text{on } S_\alpha\\
\boldsymbol{E} &\to \boldsymbol{E}^\infty \quad \text{as } |\boldsymbol{x}|\to\infty\\
-\nabla p+\mu\nabla^2\boldsymbol{v} &= 0\\
-\nabla\cdot\boldsymbol{v} &= 0\\
\boldsymbol{v} &= \boldsymbol{U}_\alpha-\frac{\epsilon\zeta_\alpha}{\mu}\boldsymbol{E}+\boldsymbol{\omega}\times(\boldsymbol{x}-b\boldsymbol{x}_\alpha) \quad \text{on } S_\alpha\\
\boldsymbol{v} &\to 0 \quad \text{as } |\boldsymbol{x}|\to\infty.
\end{aligned}$$

The boundary condition on $\boldsymbol{v}$ consists of the rigid-body motion plus the Smoluchowski slip velocity seen by an observer in the outer region beyond the thin double layer (see Section 5.7).

As in the hydrodynamic problems discussed earlier in this chapter, this problem can be solved by the method of reflections, with each reflection contribution calculated by an application of the Faxén law to the disturbance field produced by distant particle(s). The Faxén law for the electrophoretic velocity of a particle in an ambient velocity field $\boldsymbol{v}^{Amb}$ and electric field $\boldsymbol{E}^{Amb}$ has been derived by Keh and Anderson [42] as

$$\boldsymbol{U}=\frac{\epsilon\zeta}{\mu}\boldsymbol{E}^{Amb}|_{x=0}+\left(1+\frac{a^2}{6}\nabla^2\right)\boldsymbol{v}^{Amb}|_{x=0}\ . \tag{8.9}$$

Here, we temporarily use "*Amb*" instead of ∞ to denote the ambient field to avoid confusion with the widely accepted notation $\boldsymbol{E}^\infty$ for the applied electric field. Clearly, Equation 8.9 is simply the usual Faxén relation for Stokes flow, but with an effective Stokes ambient velocity field consisting of the true physical ambient field plus the Smoluchowski slip velocity. (The Faxén curvature term vanishes identically for the electric field.)

We expand the velocity and electric fields as

$$\begin{aligned} \boldsymbol{v} &= \boldsymbol{v}_1 + \boldsymbol{v}_2 + \boldsymbol{v}_{21} + \boldsymbol{v}_{12} + \cdots \\ \boldsymbol{E} &= \boldsymbol{E}^\infty + \boldsymbol{E}_1 + \boldsymbol{E}_2 + \boldsymbol{E}_{21} + \boldsymbol{E}_{12} + \cdots \ , \end{aligned}$$

with the subscripts tracing the reflection pattern as before. The zeroeth reflection at sphere 1 is the single particle result:

$$\begin{aligned} \boldsymbol{U}_1^{(0)} &= \frac{\epsilon\zeta_1}{\mu}\boldsymbol{E}^\infty \\ \boldsymbol{E}_1 &= -\frac{1}{2}\left(\frac{a}{r_1}\right)^3 (3\boldsymbol{e}_{r1}\boldsymbol{e}_{r1} - \boldsymbol{\delta}) \cdot \boldsymbol{E}^\infty \ . \end{aligned}$$

On S_1, the disturbance velocity field $\boldsymbol{v}_1$ satisfies the boundary condition,

$$\boldsymbol{v}_1 = \boldsymbol{U}_1^{(0)} - \frac{\epsilon\zeta_1}{\mu}\boldsymbol{E} = \frac{\epsilon\zeta_1}{\mu}(\boldsymbol{E}^\infty - \boldsymbol{E}) = -\frac{\epsilon\zeta_1}{\mu}\boldsymbol{E}_1 \ .$$

Since $\boldsymbol{E}_1$ is a vector harmonic, *an extension of this condition throughout the fluid region trivially gives the velocity field that satisfies the Stokes equations (with zero pressure gradient) and the above boundary condition*, so we have the desired result:

$$\boldsymbol{v}_1 = \frac{\epsilon\zeta_1}{\mu}\left[\frac{1}{2}\left(\frac{a}{r_1}\right)^3 (3\boldsymbol{e}_{r1}\boldsymbol{e}_{r1} - \boldsymbol{\delta}) \cdot \boldsymbol{E}^\infty\right] \ .$$

The disturbance field is a degenerate Stokes quadrupole and decays far away from the sphere as r^{-3}.

The first reflection at sphere 2 gives the leading order effect of hydrodynamic interactions, and this contribution is evaluated by appling the Faxén law of Keh and Anderson, Equation 8.9, to the incident electric and velocity fields:

$$\begin{aligned} \boldsymbol{U}_2^{(1)} &= \frac{\epsilon\zeta_2}{\mu}\boldsymbol{E}_1|_{x=x_2} + \left(1 + \frac{b^2}{6}\nabla^2\right)\boldsymbol{v}_1|_{x=x_2} \\ &= \frac{\epsilon\zeta_2}{\mu}\boldsymbol{E}_1|_{x=x_2} - \frac{\epsilon\zeta_1}{\mu}\boldsymbol{E}_1|_{x=x_2} \\ &= \frac{\epsilon}{\mu}(\zeta_2 - \zeta_1)\boldsymbol{E}_1|_{x=x_2} \ . \end{aligned}$$

The electrophoretic velocity to these leading order terms is thus given by

$$\boldsymbol{U}_2 = \frac{\epsilon\zeta_2}{\mu}\boldsymbol{E}^\infty - \frac{\epsilon}{\mu}(\zeta_2 - \zeta_1)\left[\frac{1}{2}\left(\frac{a}{R}\right)^3 (3\boldsymbol{dd} - \boldsymbol{\delta}) \cdot \boldsymbol{E}^\infty\right] \ .$$

We can readily generalize this result to all reflection orders and state that spheres with thin double layers do not interact hydrodynamically, unless they differ in surface potential, in which case they interact rather weakly as R^{-3}, *via* their degenerate Stokes quadrupole fields.

8.6.2 Multiple Ellipsoids

We may extend the analysis of Chen and Keh [6] to ellipsoids, including the important case of oblate (disk-like) spheroids, by combining the singularity solutions of Chapter 3 with the preceding line of reasoning. The Faxén law can be written immediately as

$$\boldsymbol{U} = \int_E f_{(1)} \left\{1 + \frac{1}{2}c^2 q^2 \nabla^2\right\} \left\{\boldsymbol{v}^{Amb} + \frac{\epsilon\zeta}{\mu}\boldsymbol{E}^{Amb}\right\} dA \ ,$$

with the ambient velocity and electric fields evaluated at the focal ellipse. If $\nabla^2 \boldsymbol{v} = 0$, as is the case with the incident fields, then the Faxén relation simplifies to

$$\boldsymbol{U} = \int_E f_{(1)} \left\{\boldsymbol{v}^{Amb} + \frac{\epsilon\zeta}{\mu}\boldsymbol{E}^{Amb}\right\} dA \ .$$

The disturbance electric field $\boldsymbol{E}_1$ produced by ellipsoid 1 can be expressed as a singularity solution [53],

$$\boldsymbol{E}_1 = (\boldsymbol{M} \cdot \boldsymbol{E}^\infty) \cdot \nabla\nabla \int_E \frac{f_2(\boldsymbol{\xi})\, dA(\boldsymbol{\xi})}{|\boldsymbol{x} - \boldsymbol{\xi}|} \ ,$$

where $\boldsymbol{M}$ is a diagonal tensor expressible in terms of elliptic integrals, *viz.*,

$$M_{ii} = \left[\frac{3}{abc} - \frac{3}{2}\int_0^\infty \frac{dt}{(a_i^2 + t)\Delta t}\right]^{-1} \qquad \text{(no sum on } i\text{)}.$$

By following the same path as in the discussion for spheres, we find the following expression for the electrophoretic velocity of ellipsoid 2:

$$\boldsymbol{U}_2 = \frac{\epsilon\zeta_2}{\mu}\boldsymbol{E}^\infty + \boldsymbol{U}_2^{(1)} \ ,$$

with

$$\begin{aligned} \boldsymbol{U}_2^{(1)} &= -\frac{\epsilon}{\mu}(\zeta_2 - \zeta_1)(\boldsymbol{M} \cdot \boldsymbol{E}^\infty) \cdot \\ & \int_{E2}\int_{E1} \frac{f_{(1)}(\boldsymbol{\xi}_2) f_{(2)}(\boldsymbol{\xi}_1)}{R^3} (3\boldsymbol{dd} - \boldsymbol{\delta})\, dA_1(\boldsymbol{\xi}_1) dA_2(\boldsymbol{\xi}_2) \ . \end{aligned} \qquad (8.10)$$

The separation $R(\boldsymbol{\xi}_1, \boldsymbol{\xi}_2)$ and unit vector $\boldsymbol{d}$ now denote, respectively, the distance and direction between two points $\boldsymbol{\xi}_1$ and $\boldsymbol{\xi}_2$ on the focal ellipses. The analysis of the interaction between two ellipsoids and degenerate cases (spheroids) in various configurations of interest in colloidal hydrodynamics now follows in a straightforward fashion from this general result.

Exercises

Exercise 8.1 The Force and Torque on Two Rotating Spheres.
Consider two stationary spheres centered at $\boldsymbol{x}_1$ and $\boldsymbol{x}_2$ undergoing independent rotational motions, $\boldsymbol{\omega}_1 \times (\boldsymbol{x} - \boldsymbol{x}_1)$ and $\boldsymbol{\omega}_2 \times (\boldsymbol{x} - \boldsymbol{x}_2)$, in a quiescent fluid. Use the method of reflections to calculate the force and torque on the spheres accurate to $O(R^{-6})$.

Exercise 8.2 The Force on Two Translating Spheres.
Extend the results of Example 8.1 to $O(R^{-6})$ by including contributions from the fifth and sixth reflections. Note that the quadrupole terms in $\boldsymbol{v}_{12}$ and $\boldsymbol{v}_{21}$ must be retained so that the Faxén relation for the quadrupole moment,

$$\begin{aligned}\oint_S (\boldsymbol{\sigma}\cdot\hat{\boldsymbol{n}})_i \xi_j \xi_k \, dS(\boldsymbol{\xi}) &= C_1 \pi \mu a^5 \left\{1 + \frac{a^2\nabla^2}{14}\right\} \boldsymbol{v}^\infty(\boldsymbol{x})_{i,jk}|_{x=0} \\ &+ C_2 a^2 F_i \delta_{jk} + C_3 a^2 (F_j \delta_{ik} + F_k \delta_{ij}) \ ,\end{aligned}$$

must be derived. The method devised in Chapter 3 may be used [43], or, in this case, some simple arguments to fix the constants C_1, C_2 and C_3. Compare your answer for the force with the result given in Chapter 11.

Exercise 8.3 Sedimentation of Three Spheres.
Consider the mobility version of the three-sphere example: three identical, torque-free spheres with centers at $\boldsymbol{x}_1$, $\boldsymbol{x}_2$, and $\boldsymbol{x}_3$, settling under the action of gravity. To reduce the number of parameters, consider centers at the vertices of an equilateral triangle, so that $|\boldsymbol{x}_\alpha - \boldsymbol{x}_\beta| = R$ for all α, β. Find the sedimentation velocities accurate to $O(R^{-5})$ using just two reflections.

Exercise 8.4 External Torques on Two Spheres.
Consider two spheres with external torques acting about $\boldsymbol{x}_1$ and $\boldsymbol{x}_2$ in a quiescent fluid. Use the method of reflections to calculate the resulting rigid-body motions accurate to $O(R^{-5})$.

Exercise 8.5 Resistance Tensors by Inversion of Mobility Tensors.
The results from the previous exercise and the mobility example given earlier in the chapter provide to $O(R^{-5})$ the complete description of the mobility tensor for two spheres. Show that the resistance tensors obtained by inversion of these results are consistent with those obtained by direct calculation.

Exercise 8.6 Two Force-Free and Torque-Free Spheres in a Linear Field.
Consider two force-free and torque-free spheres in the linear field,

$$\boldsymbol{v}^\infty = \boldsymbol{\Omega}^\infty \times \boldsymbol{x} + \boldsymbol{E}^\infty \cdot \boldsymbol{x} \ .$$

Use the method of reflections to calculate the rigid body motion and stresslet for each sphere. Compare your solution to the result given in Chapter 11. Results for the relative velocity, $\boldsymbol{U}_2 - \boldsymbol{U}_1$, and the rotational velocities are also available from [1]. Their expression for the relative velocity,

$$\boldsymbol{U}_2 - \boldsymbol{U}_1 = \boldsymbol{\Omega}^\infty \times (\boldsymbol{x}_2 - \boldsymbol{x}_1) + \boldsymbol{E}^\infty \cdot (\boldsymbol{x}_2 - \boldsymbol{x}_1) - [A\boldsymbol{dd} + B(\boldsymbol{\delta} - \boldsymbol{dd})] \cdot \boldsymbol{E}^\infty \cdot (\boldsymbol{x}_2 - \boldsymbol{x}_1) \ ,$$

with

$$\begin{aligned} A &= \frac{5}{2}\frac{a^3+b^3}{R^3} - \frac{3(a^5+b^5)+5a^2b^2(a+b)}{2R^5} + 25\frac{a^3b^3}{R^6} + o\left(\left(\frac{a+b}{R}\right)^6\right) \ , \\ B &= \frac{3(a^5+b^5)+5a^2b^2(a+b)}{3R^5} + o\left(\left(\frac{a+b}{R}\right)^6\right) \ , \end{aligned}$$

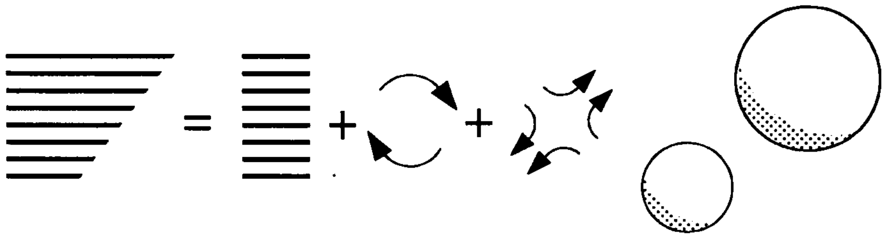

Figure 8.9: Two spheres in a linear field.

has gained wide usage. The functions A and B correspond, respectively, to motions along and transverse to the line of centers.

Exercise 8.7 Sedimentation of Two Oblate Spheroids.
Use the Faxén relations for the oblate spheroid to derive sedimentation velocities for two oblate spheroids. Compare the strength of hydrodynamic interactions with that in the corresponding problem for prolate spheroids.

Exercise 8.8 Electrophoresis of Two Oblate Spheroids.
Simplify Equation 8.10 for the case of two equal oblate spheroids. Devise a numerical scheme for the integrations over the focal ellipse and examine the electrophoretic mobility of two spheroids in edge-edge, edge-face, and face-face configurations at various orientations to the applied electric field.